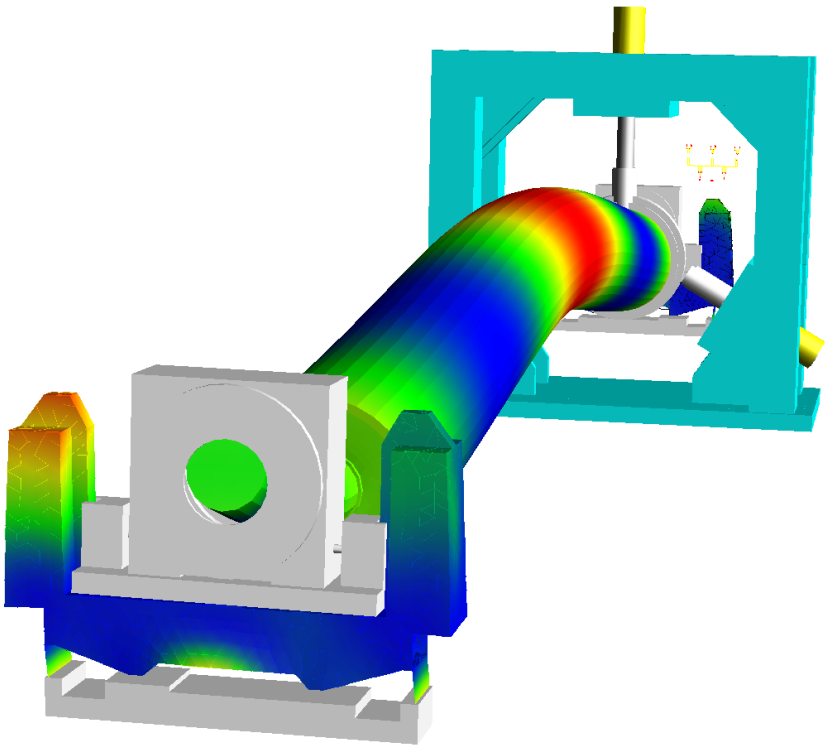

ADAMS/Simulink Simulation of Active Damping of a Heavy Roller

Customer: VTT - Intelligent Products and Systems Theme

VTT TECHNICAL RESEARCH CENTRE OF FINLAND

VTT INDUSTRIAL SYSTEMS

Public	X	Registered in VTT publications register JURE	X
Confidential until / permanently			
Internal use only			

Title

ADAMS/Simulink Simulation of Active Damping of a Heavy Roller

Customer or financing body and order date/No.	Research report No.
VTT Technical Research Centre of Finland	BTUO57-031129
Project T3SULAROTOR	Project No. H2SU00104 (TUO) E2SU00090 (ELE)
Author(s) Markku Järviluoma (VTT/ELE), Juha Kortelainen (VTT/TUO)	No. of pages/appendices 38 / 6

Keywords

control system, flexible structure, hydraulic, paper machine, roll, simulation, vibration

Summary

A dynamic model for a heavy rotating paper machine roller and a hydraulic force actuator system is modified for the simulation of active vibration damping. The model is built using ADAMS simulation software. The control system for active damping is modelled using Matlab/Simulink software and C programming. The simulated system corresponds to a real test system used in an earlier project (PYÖRIVÄRE). Some comparisons between the model and the real system are done and the main sources for the differences are found in roller unbalance and the tuning of the force feedback controllers (analogue PID:s).

The aim of active damping is to control the force generator so, that the displacements in the middle (length wise) of the roller are attenuated in the horizontal and vertical directions. The used damping control algorithms include higher harmonic control (HHC) and convergent control (CC). These both are open loop control methods, where sinusoidal control signals are synchronised according to the measured vibrations and the frequency response model of the system. The HHC damping works well both in unbalance compensation (1st harmonic damping) and in simultaneous damping of multiple harmonics. The CC damping showed in the simulations same kind of problems as it has shown in practical tests, especially considering multiple harmonics damping.

Date 11 March, 2003

Pekka Koskinen	Markku Järviluoma	
Deputy Research Manager	Senior Research Scientist	Checked

Distribution (customers and VTT):

VTT TECHNICAL RESEARCH CENTRE OF FINLAND
VTT INDUSTRIAL SYSTEMS
Otakaari 7 B, Espoo
P.O. Box 13022, FIN-02044 VTT
FINLAND
Tel. +358 9 4561
Fax +358 9 456 5888
name.surname@vtt.fi
www.vtt.fi/tuo
Business ID 0244679-4

Table of contents

1 Introduction

Active damping of vibration of a rotating roller was one topic in the project PYÖRIVÄRE (1999-2002). A test set-up consisting of a 5 meter long paper machine roller (weight 800 kg) and a hydraulic external force actuator was designed and built in the laboratory of Machine Design at Helsinki University of Technology. The hydraulic actuator consisted of three cylinders, which were controlled with servo valves. Cylinder forces were controlled with analogue feedback (PID) from measured cylinder pressures. The forces were transmitted to the rotating roller via an extra third bearing near the free end of the roller. In active damping tests ball bearings were used both as supporting bearings and the extra bearing. The test set-up and the results from active damping tests are described in the report [Järviluoma & Valkonen 2002].

Also an ADAMS model of the roller and the force actuator system was developed during PYÖRIVÄRE in the Mechanical Engineerin Department of Lappeenranta University of Technology. These models are described in reports [Sopanen 2002] and [Kemppainen 2001]. These models were used for studying the properties of the rotor and how they are affected by various design parameters and properties of e.g. the supporting bearing types. The simulation of active damping was also tried in VTT Automation but it failed due to too high complexity of the simulation model. For that purpose the model was modified and simplified at VTT Industrial Systems as part of SULAROTOR project. These modifications are described in Section 2 in this report.

The control system for the active damping is simulated with Simulink software and the ADAMS model of the roller and the actuators are included as a block in the Simulink model. The damping algorithms are coded with C and included in the model as dll-functions. This model is described in Section 3 in this report.

Simulation of the force feedback controllers (analogue PID) is presented in Section 4. The PID-controllers are tuned manually by observing the step responses of the force control loops while the roller is not rotating. The vibration spectrums of the system with rotation speeds ranging over the half critical speed are compared to the ones measured from the real system in Section 5. The comparison is done both when there is contact between the cylinder piston rods and the third bearing (cylinders closed, positive force set-values) and when there is no contact (cylinders open, negative force set-values).

Simulation results from the actual active damping are presented in Sections 6 and 7. The simulated damping algorithms are the Higher Harmonic Control (HHC) and Convergent Control (CC), which was used also in PYÖRIVÄRE tests.

2 Mechanical System Simulation Model

The modified simulation model is shown in Figure 1. The following changes were made to the original simulation model

- all three detailed bearing structures (free and driving end bearing of the roll and the vibration damper bearing) were replaced with simple ideal point-to-curve or spherical joint constraints,

- the original hydraulic subsystem that was modelled using the AXO macros was replaced with simplified hydraulic subsystem modelled using ADAMS/Hydraulics components (see Section 2.2),
- instead of setting the damping ratios of flexible parts using FORTRAN subroutines the damping ratios were set using function expressions; all the damping coefficients were preserved and
- unused design variables and markers were removed to clean up the model.

Mass properties of all the parts in the model were preserved. The parts of the model and their mass properties are shown in Appendix A. Four tool command files were included into the simulation system to allow the user to remove and add the flexibility of the bearing and vibration damper frames.

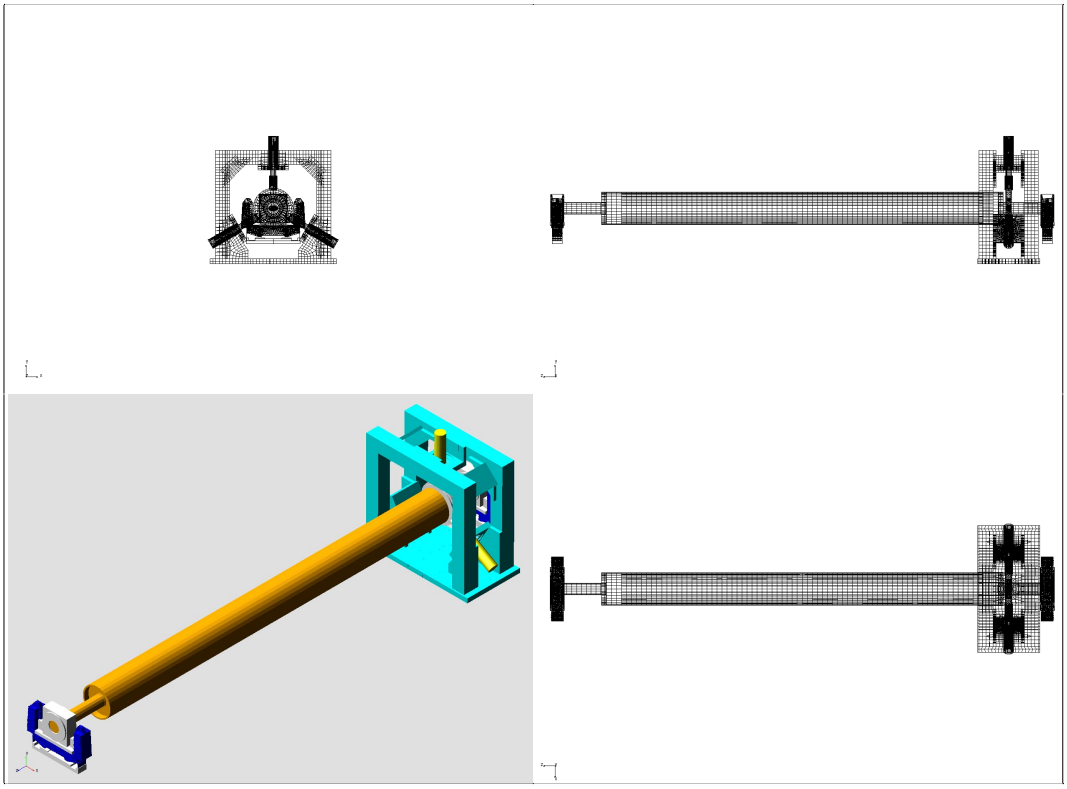

Figure 1: Modified simulation model.

2.1 Flexible Parts

The simulation model includes the following flexible parts

- roll,
- the frame of the free end bearing,
- the frame of the driving end bearing and
- the frame of the vibration damper.

The software version of ADAMS used to create the original simulation model didn't include possibility to describe the damping ratios of a flexible part using function expressions but the damping ratios had the be set using FORTRAN subroutine. In the modified simulation model the damping ratios of the flexible parts were set using function expressions. The ratios are the same used in the original model (see Table 1).

Four tool command files were created to simplify the testing and development of the control system of the damper hydraulic subsystem. With these command files user can turn off and on flexibility of flexible parts (excluding the roll).

Table 1: Relative damping ratios of the flexible parts.

	Frequency [Hz]	Relative damping ratio
Roll	0 - 100	0,018 %
	100 - 210	0,016 %
	210 - 300	0,023 %
	300 - 1600	0,720 %
	1600 -	100,000 %
Bearing frames	0 - 400	10,610 %
	400 - 500	6,610 %
	500 - 4000	20,000 %
	4000 - 7000	10,000 %
	7000 -	100,000 %
Vibration damper	0 - 100	1,000 %
	100 - 1000	10,000 %
	1000 -	100,000 %

2.2 Hydraulic Subsystem

The modelled hydraulic subsystem of the damper is shown in Figure 2. The subsystem was modelled using ADAMS/Hydraulics package. The subsystem includes the following components:

- fluid component (physical properties of the hydraulic fluid)
- pressure source
- input side flow sum component (junction)
- three servo valves
- three hydraulic cylinders
- tank side flow sum component (junction)
- tank

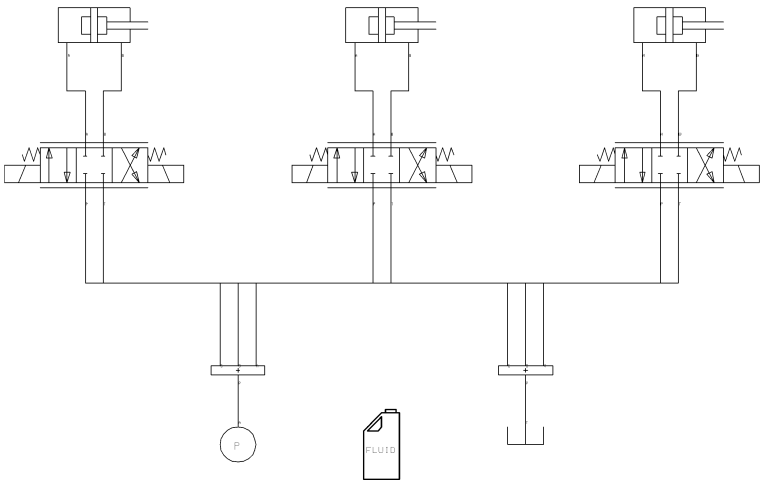

Figure 2: The modelled hydraulic subsystem.

2.3 Control System Interface

The control system interface is illustrated in Figure 3. The control system of the roller damper hydraulic subsystem was modelled using Matlab Simulink software. For the control system nine input and three output variables were defined in the mechanical system model (see Table 2).

In the real world roller measuring horizontal and vertical location of the centre point of the roll would have been done by measuring the surface of the roll. This was not possible in the model using function expressions and would have required some extra work to be done using a FORTRAN subroutine. In ADAMS only node points of a flexible part can be used as a measure point of location. Because the roll was hollow inside the horizontal and vertical location of the centre point had to be calculated as an average of locations of points at perimeter of the centre cross section of the roll (see Figure 4). The used method filters out the effects of roll deformation but gives quite a good estimation of location of the roll centre point.

One way to implement the roll centre point measurement in the model would be to fit a spline curve on a set of roll surface points and then calculate the distance of the fitted curve from a measurement point (location of a sensor). The curve could be fitted locally for horizontal and vertical measurement.

Table 2: The control system interface variables in the mechanical system model.

	Interface Inputs/Outputs	Interface Variable
Control System Inputs:		
1	Horizontal location of the roll center point	VAR_asema_x
2	Vertical location of the roll center point	VAR_asema_y
3	Roll rotational speed	VAR_pyorimisnopeus
4	Hydraulic pressure of the cylinder 1 at the load side	VAR_sylinteri_1_p_A
5	Hydraulic pressure of the cylinder 1 at the unload side	VAR_sylinteri_1_p_B
6	Hydraulic pressure of the cylinder 2 at the load side	VAR_sylinteri_2_p_A
7	Hydraulic pressure of the cylinder 2 at the unload side	VAR_sylinteri_2_p_B
8	Hydraulic pressure of the cylinder 3 at the load side	VAR_sylinteri_3_p_A
9	Hydraulic pressure of the cylinder 3 at the unload side	VAR_sylinteri_3_p_B
Control System Outputs:		
A	Control input for the hydraulic cylinder 1 servo valve	VAR_servo_1
B	Control input for the hydraulic cylinder 2 servo valve	VAR_servo_2
C	Control input for the hydraulic cylinder 3 servo valve	VAR_servo_3

2.4 Natural Frequencies

The damped natural frequencies of the simulation model are listed in a table in Appendix B. There were a set pressure of 10 bars in the hydraulic system and all servo valves were closed during the eigen mode analysis. Some of the damped eigen modes of the model are described in Table 3.

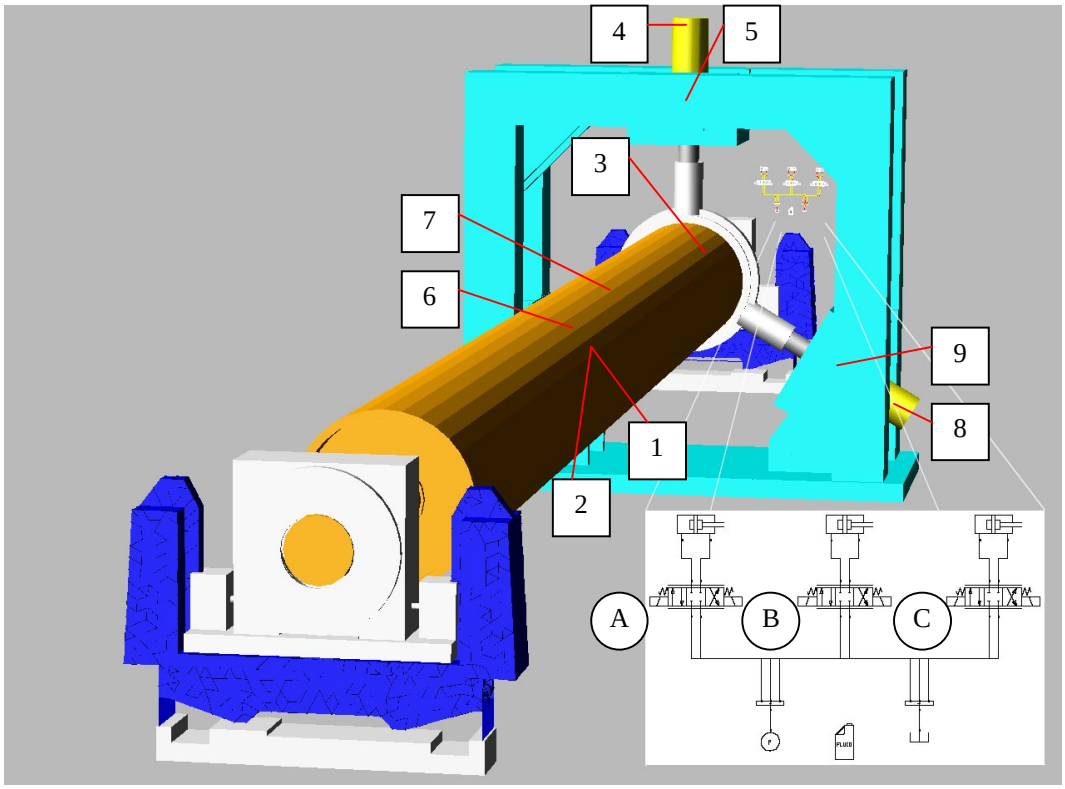

Figure 3: The control system interface in the model.

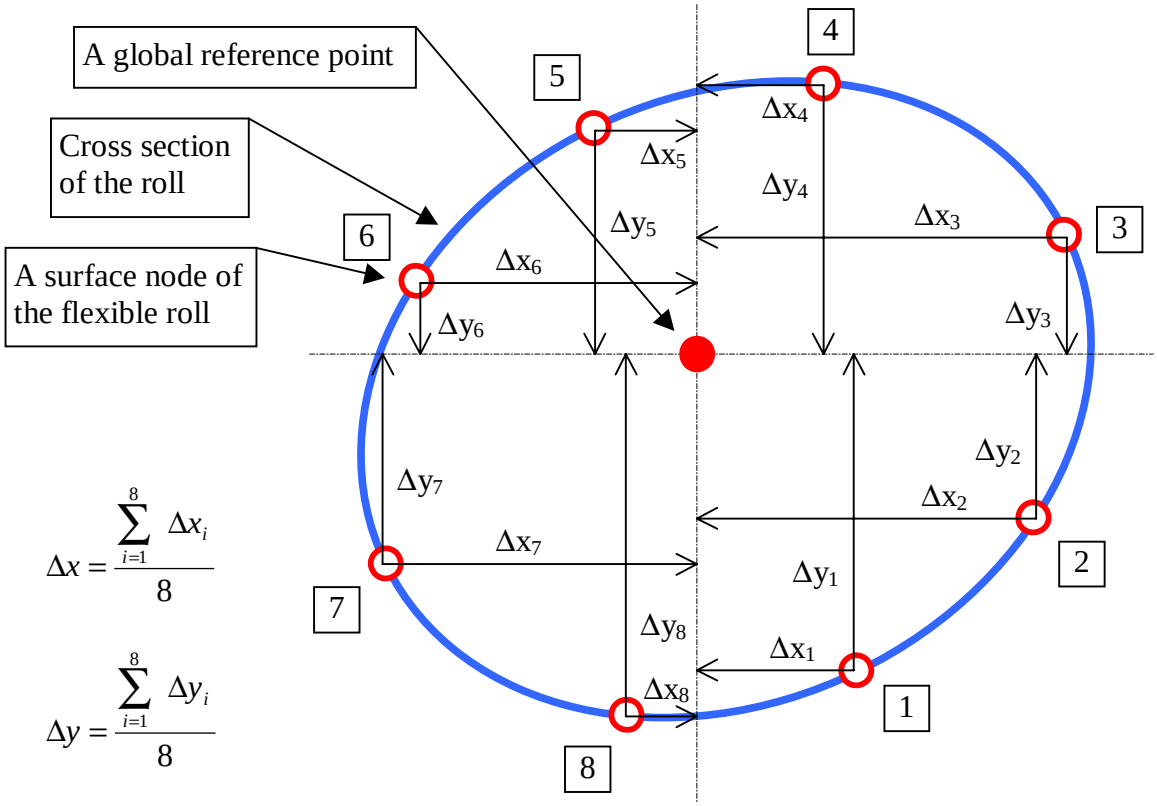

Figure 4: The method used in the model to get the location of the roll centre point. The used method of getting the location of the roll centre point tends to filter out shape deviations of the cross section of the roll.

Table 3: Description of some undamped eigenmodes of the model.

Mode	Frequency [Hz]	Mode Description
24	28,5	The first roll benging shape, horizontal
25	29,5	The first roll benging shape, vertical
26	65,3	The second roll benging shape, horizontal
27	72,8	The second roll benging shape, vertical
28	83,6	Axial translation of the roll, the vibration damper and bearing frames bend
29	87,6	Translation of the hydraulic cylinder in roll axial direction
30	118,2	The third roll benging shape, horizontal
31	120,8	Lateral benging of the vibration damper
32	123,6	Rotation of the bearing sleeve
33	127,7	Rotation/translation of the hydraulic cylinder around the top cylinder axis
34	133,6	The third roll benging shape, vertical
35	150,0	No visual feedback. The eigenfrequencies of servo valves in the model are set to 150 Hz
36	150,0	No visual feedback. The eigenfrequencies of servo valves in the model are set to 150 Hz
37	150,0	No visual feedback. The eigenfrequencies of servo valves in the model are set to 150 Hz
38	158,7	Lateral bending of the bearing frame of the driving end
39	185,1	Lateral bending of the bearing frame of the free end
40	207,8	Longitudinal translation of the pistons of the hydraulic cylinders

2.5 Model Units and Simulation Settings

ADAMS is a unit sensitive solver for mechanical systems. This means that the selected unit set has an influence to the robustness of the simulation and in some case to the accuracy of the solution. Therefore some experiments were done to find out the most convenient unit set so that the simulation time and robustness of the model were optimised in some level. The used unit set is shown in Table 4.

Table 4: The unit set used in the model.

Length	meter
Angle	degree
Force	kilonewton
Mass	kilogram
Time	millisecond
Frequency	Hertz

The default integrator in the model was set to GSTIFF and the option for equation formulation was set to SI2 (Stabilized-Index Two). This with the maximum integrator time step set to value 0.1 ms stabilized the integrator and the test simulations ran robustly.

3 Simulink Model of the Control System

The control system of the hydraulic actuator system was modelled in Simulink environment. The Simulink simulation is done with fixed-step integration using step size 0.5 ms and Dormand-Prince (ode5) integrator. The time scale in the model is milliseconds, which affects all parameter values e.g. in continuous time filters.

The highest level of the control system is shown in Figure 5. The ADAMS model is included as one block (adams_sub) and it operates in discrete batch mode with 0.5 ms communication interval. The inputs to the ADAMS model (u1, u2 and u3) are the control signals to the servo valve models, scaled between -1 and +1. The vibration measurements from the roller are obtained as displacements of the roller centre point (length wise in the middle of the roller) in horizontal (x) and vertical (y) directions, the scale is meters. The out of roundness of the roller surface does not show in the displacement measurements. The rotation speed of the roller is obtained in rad/ms. The oil pressures in the cylinders are measured from the both sides of the piston in kN/m2.

The Pressure measurements are converted to cylinder forces in the block 'Pressures → Forces', see Figure 6. The conversion is done simply as $F = P_A A_A - P_B A_B$. The analogue force feedback controllers are included in the block 'Force PID', see Figure 7. The set value signals for the force feedback controllers are obtained from the 'Damping controller' block, see Figure 8, which includes the damping algorithms as dll-subroutines written with C-language. The clock inputs to this dll-block are used for timing, the damping algorithm is executed once per control interval, which is set to be 1 ms. Between these events the outputs from this block are constants (zero order hold).

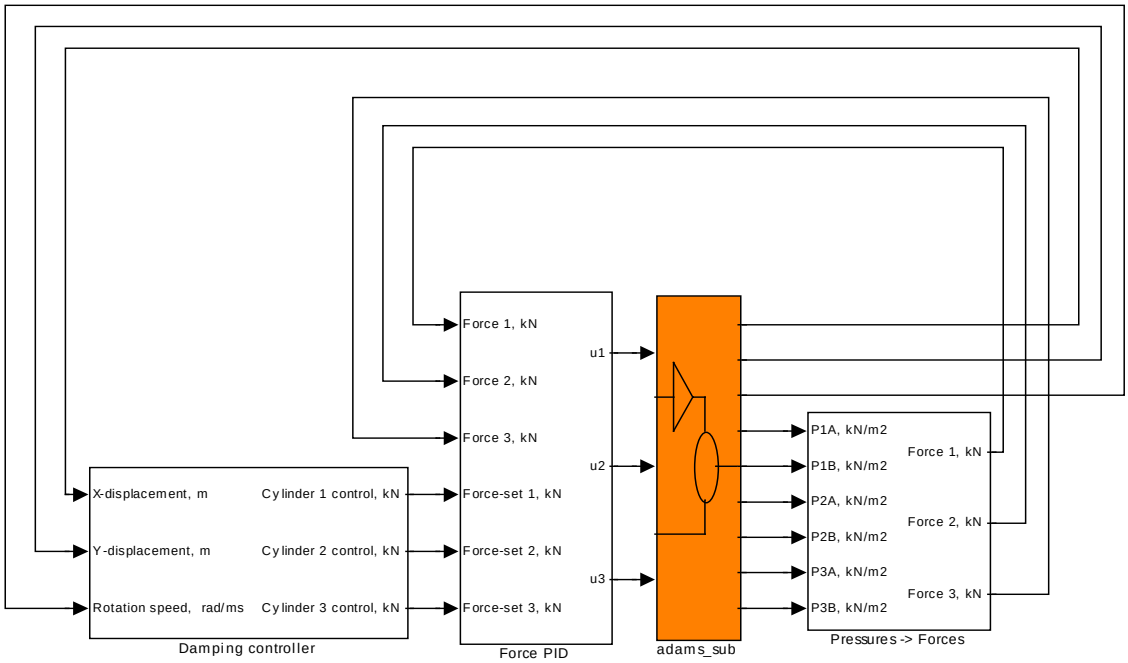

Figure 5: Highest level Simulink model.

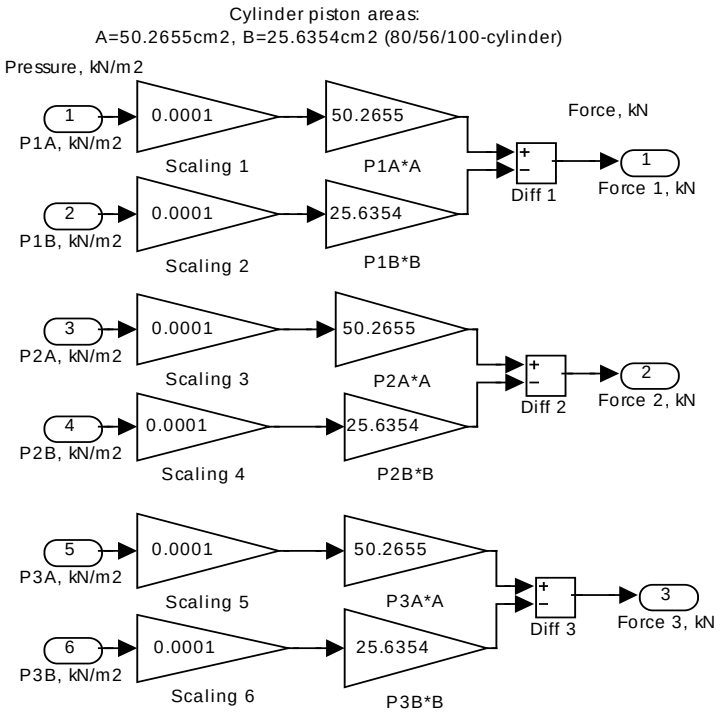

Figure 6: Pressures to forces conversion block.

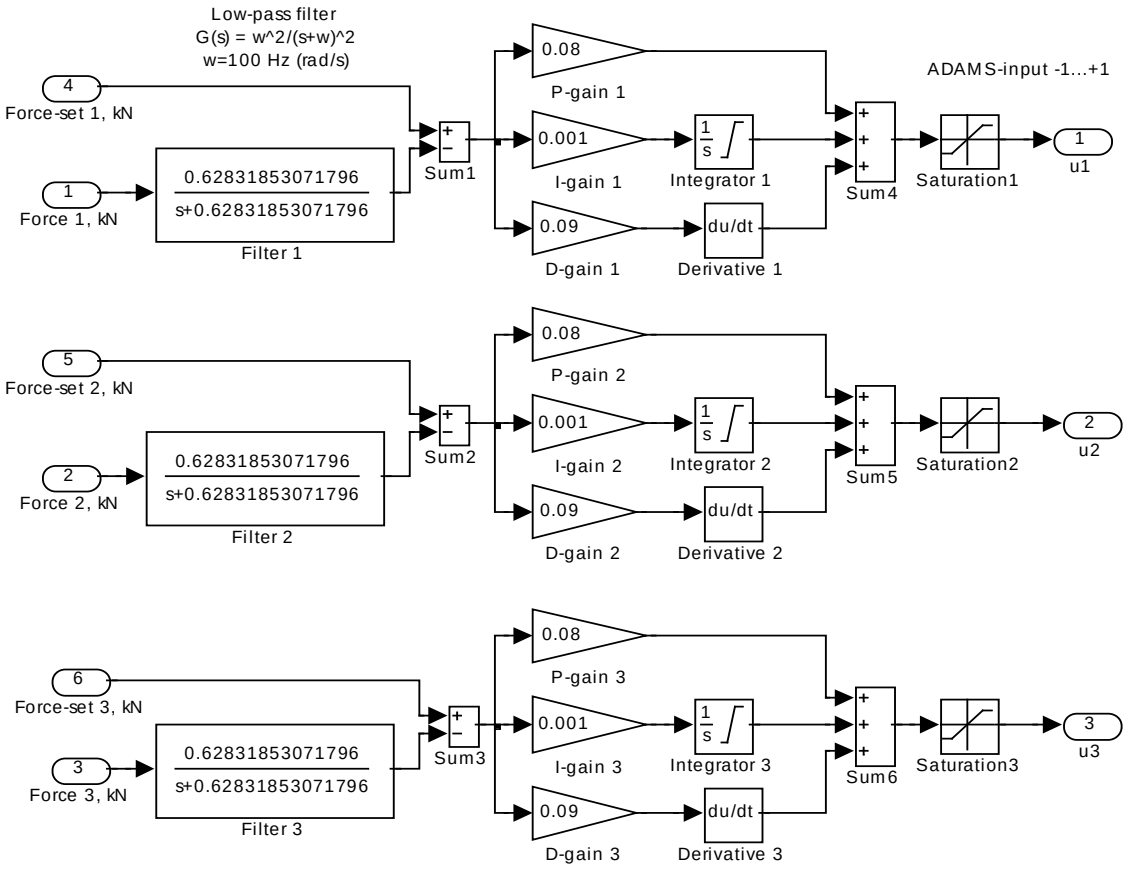

Figure 7: Force feedback controller block.

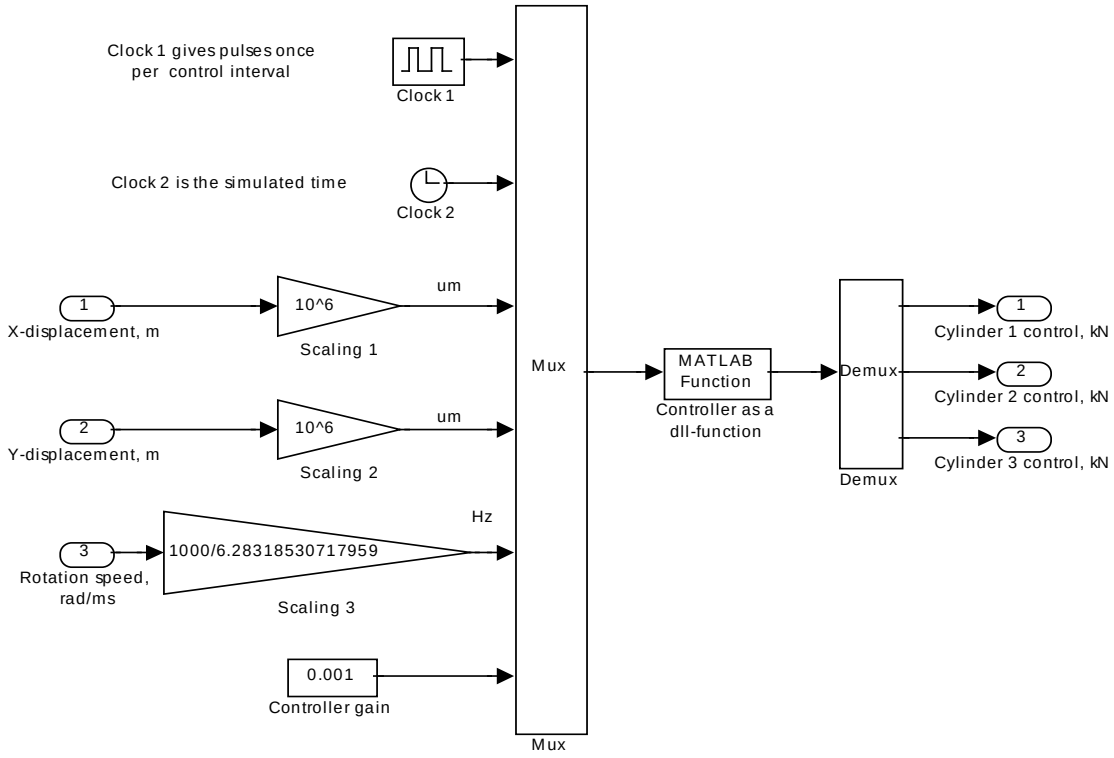

Figure 8: Damping controller block.

4 Tuning of the Force Feedback Control

4.1 Analogue PID Force Control of Each Cylinder

The analogue force feedback controllers were tuned manually by trial and error. The rotation speed was zero and all three cylinders got a step set value change simultaneously. The best tuning is shown in Figure 9. No numerical criteria was used in tuning, the gains were set so that the rise time is as small as possible without considerable overshoot. Same practical approach was used also when tuning the force controllers in the real test bench during PYÖRIVÄRE project.

The frequency responses of the force feedback loops of each of the three cylinders were measured using a noise test signal. The test signal and its spectrum are shown in Figure 10. This test signal was fed as the set value signal separately for each cylinder controller while the other two cylinders had a constant set value of 2 kN. The forces of each of the three cylinders are measured in all tests so that also the cross couplings can be observed.

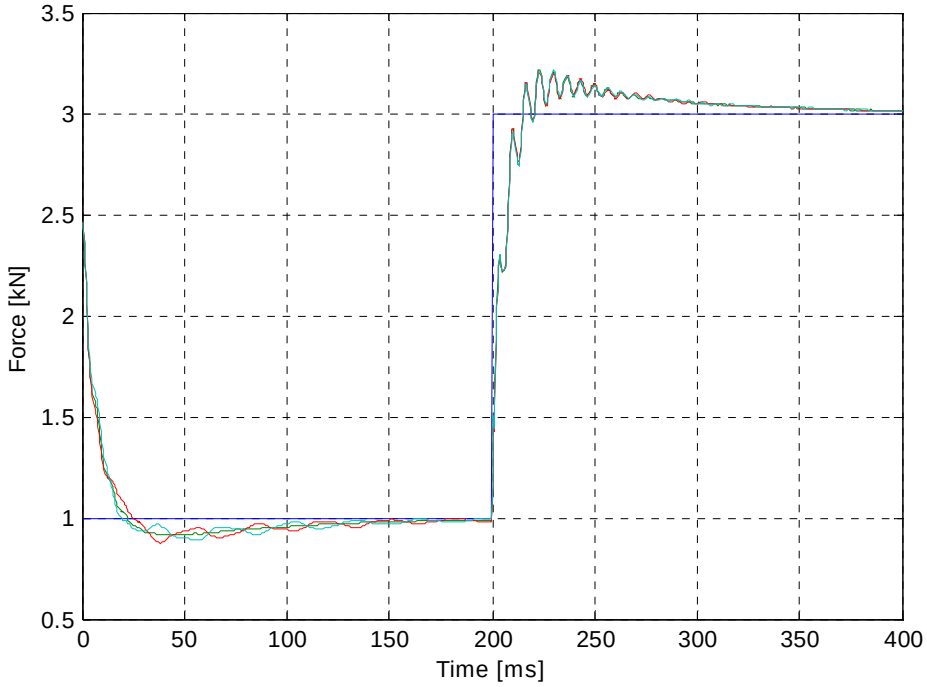

Figure 9: Step responses of the force feedback loops with PID-gains P=0.08, I=0.001, D=0.09. All three responses are plotted on top of each other. The set value changes from 1 kN to 3 kN at time 200 ms.

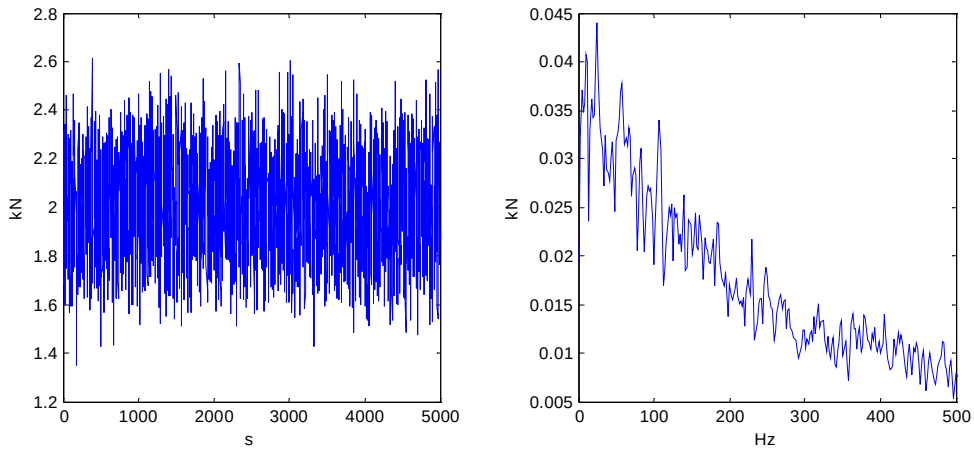

Figure 10: Noise test signal.

The measured frequency responses are shown in Figure 11 (gain curves) and Figure 12 (phase curves). There are cross couplings to some extent. The natural frequencies of the roller can be seen especially at frequencies below 100 Hz. The high peaks at about 150 Hz are caused by the hydraulic system. In the ADAMS model the nominal frequencies of the servo valves are set to 150 Hz and the damping ratios to 10 %. This damping ratio is probably too low, a value between 50–70 % would be closer to reality. However, the main interest is in the frequencies below 100 Hz so that this is not considered significant. In Figure 13 are shown the coherence curves from the noise tests. The coherence is reasonable in the diagonal cases. The cross coupling measurements are somewhat more uncertain at low frequencies and at the roller resonance frequencies.

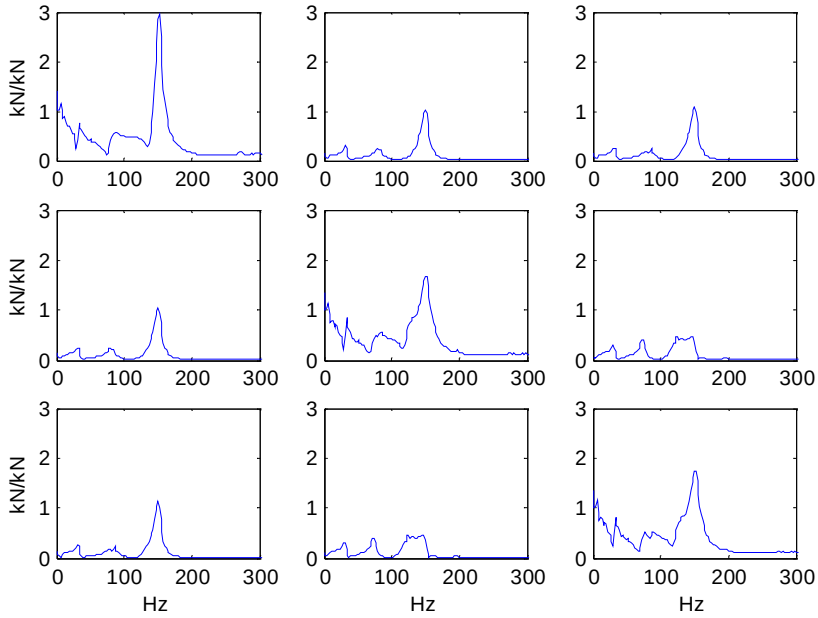

Figure 11: The gain curves of the force PID control loops. In the top row the noise set value signal is used for cylinder 1, in the middle row it is used for cylinder 2 and in the bottom row for cylinder 3. In the left column is the force response in cylinder 1, in the middle column the response of cylinder 2 and in the right column cylinder 3.

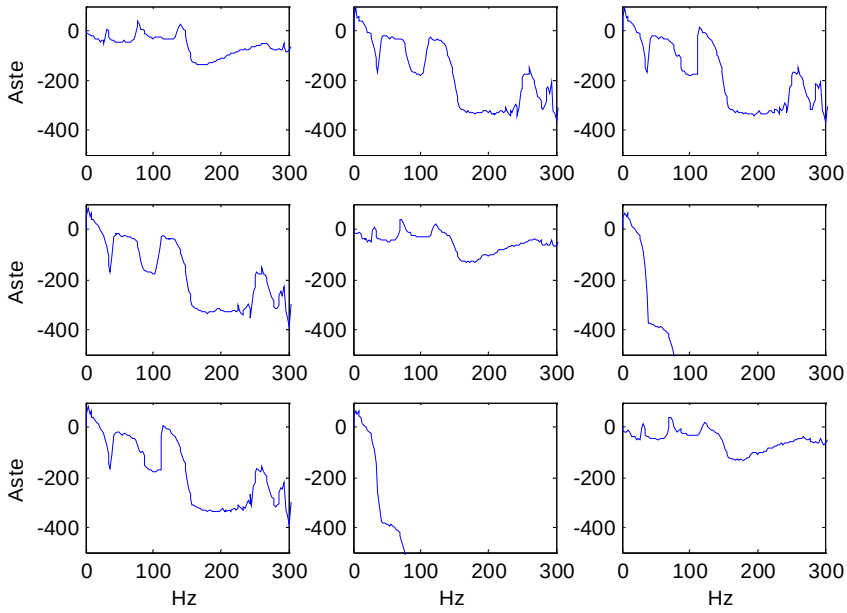

Figure 12: The phase curves of the force PID control loops.

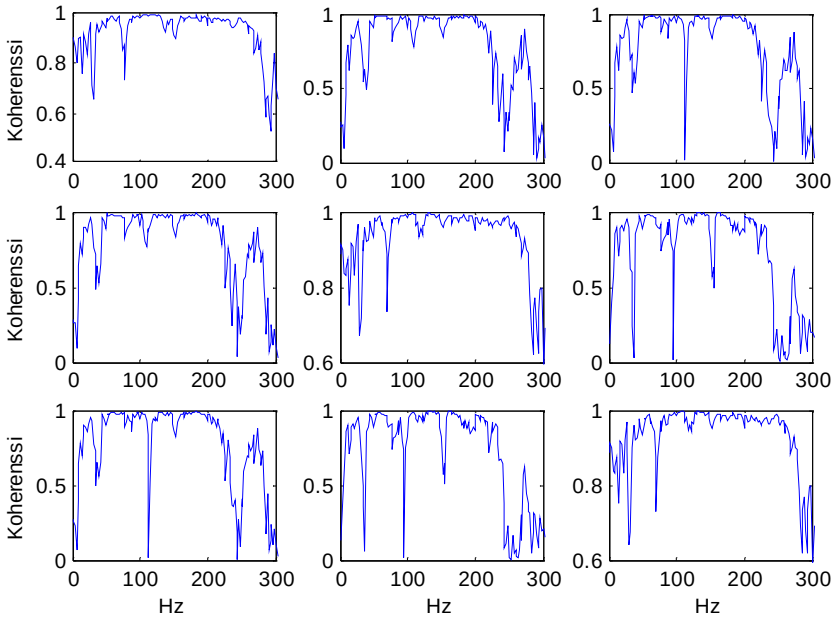

Figure 13: The coherence curves of the frequency response measurement tests.

4.2 Horizontal and Vertical Force Generation

The aim of active damping in this case is to attenuate or reject vibrations at the middle (length wise) of the roller in two dimensions, horizontal (x) and vertical (y). Hence, there are two output variables and, so far, three control variables (the force set value signals to the three cylinders). This excess of control inputs makes the design of control algorithms for active damping difficult, there is not enough information to exactly define all inputs. However, there is an additional restriction for the inputs: the cylinder forces must all the time be positive with some margin, otherwise the contact between the actuator and the roller would be lost and disturbing force impacts would follow.

In order to make the system a 2 by 2 multivariable system and to keep the cylinder forces positive, the force set values are defined in two dimensions, horizontal and vertical. If these forces are F_x and F_y, then according to Figure 14

$$F_x = -CF_2 + CF_3 \tag{1}$$

$$F_y = -F_1 + SF_2 + SF_3 \tag{2}$$

where C is $\cos(30°) = \sqrt{3}/2$ and S is $\sin(30°) = 1/2$.

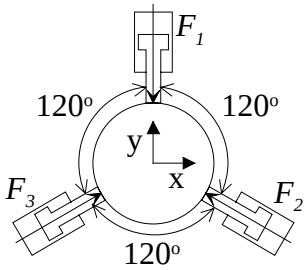

Figure 14: The cylinder forces.

One way to preserve a minimum force F_{min} for all cylinders is to divide the horizontal and vertical forces F_x and F_y to the three cylinders in the way described in Table 5. This method will keep at least one of the cylinders at the minimum force and others at higher forces and should produce as small forces as possible. In Figure 15 is shown an example of the generation of the three cylinder force set values from the set values for horizontal and vertical forces. This is a non-linear filter ('blending filter') and, as can be seen from Figure 15, it generates higher harmonic components for the individual cylinder forces. An other possibility is to use so high average forces for all three cylinders so that horizontal and vertical forces can be generated both in negative and positive directions without reaching low limit for individual cylinder forces.

Table 5: Generation of horizontal and vertical force set values by preserving minimum forces for all cylinders.

$A = F_2 - F_1 = F_y - \frac{1}{\sqrt{3}} F_x$ and $B = F_3 - F_1 = F_y + \frac{1}{\sqrt{3}} F_x$			
$A < B$		$A \geq B$	
$A \geq 0$	$A < 0$	$B \geq 0$	$B < 0$
$F_1 = F_{min}$ $F_2 = F_1 + A$ $F_3 = F_1 + B$	$F_2 = F_{min}$ $F_1 = F_2 - A$ $F_3 = F_1 + B$	$F_1 = F_{min}$ $F_3 = F_1 + B$ $F_2 = F_1 + A$	$F_3 = F_{min}$ $F_1 = F_3 - B$ $F_2 = F_1 + A$

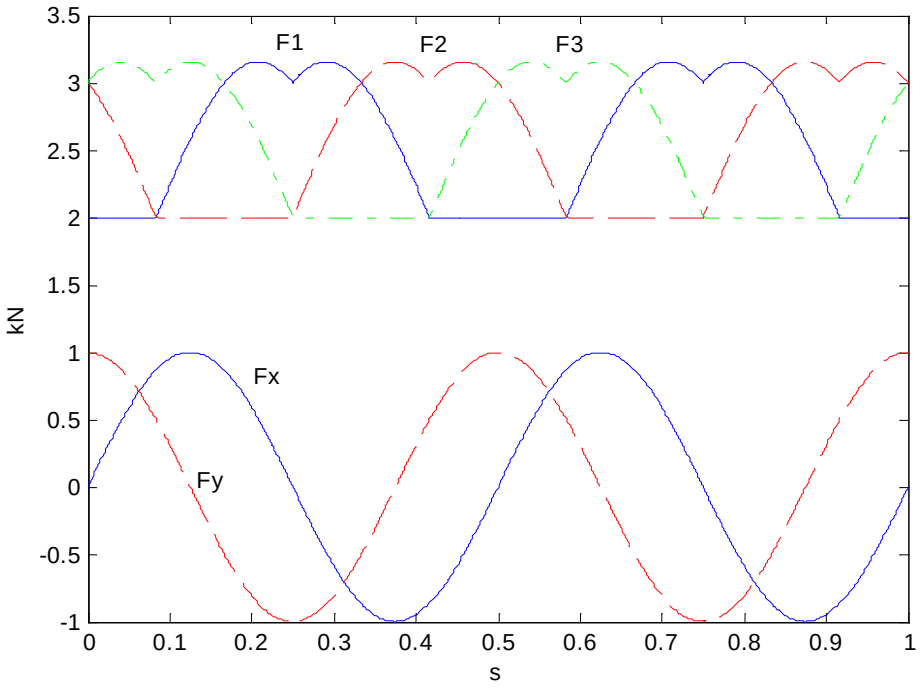

Figure 15: An example of dividing force set values Fx ja Fy to the three cylinders so, that a minimum force of 2 kN is preserved for all cylinders.

The frequency responses of the horizontal and vertical force control were measured using the same noise test signal as before. There were two test runs in which the noise test signal was used either as horizontal or vertical force set value while the other direction was kept at zero.

The results are presented in Figure 16 and Figure 17. The cross couplings are negligible. The coherence curves are shown in Figure 18.

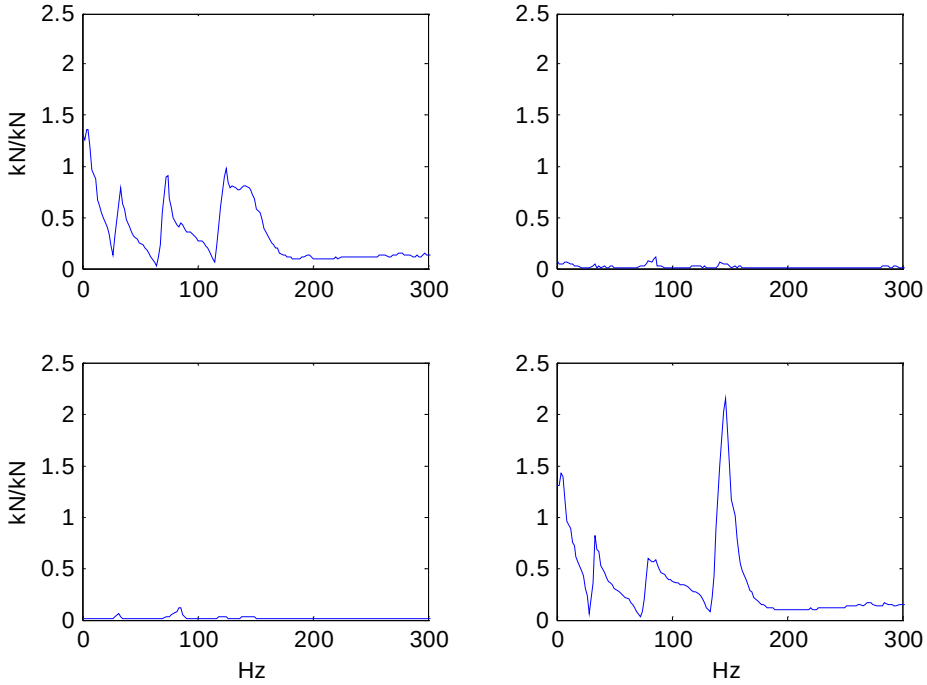

Figure 16: The gain curves of the measured (simulation) frequency responses of horizontal and vertical force control. Horizontal control is in the top row and vertical control at the bottom row. Horizontal force response is at left and vertical force response at right.

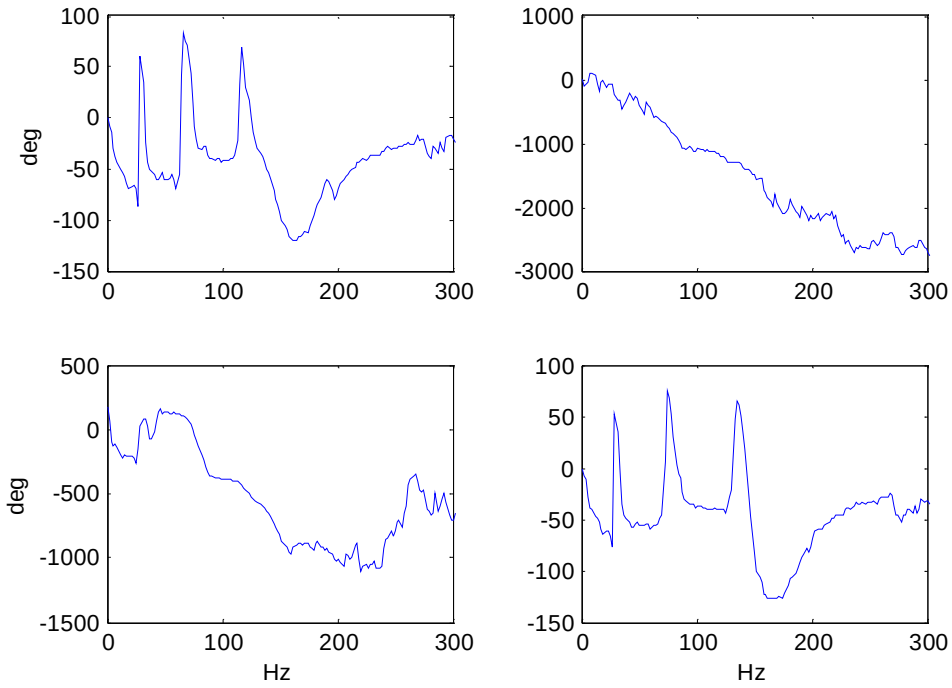

Figure 17: The phase curves of the measured (simulation) frequency responses of horizontal and vertical force control. Horizontal control is in the top row and vertical control at the bottom row. Horizontal force response is at left and vertical force response at right.

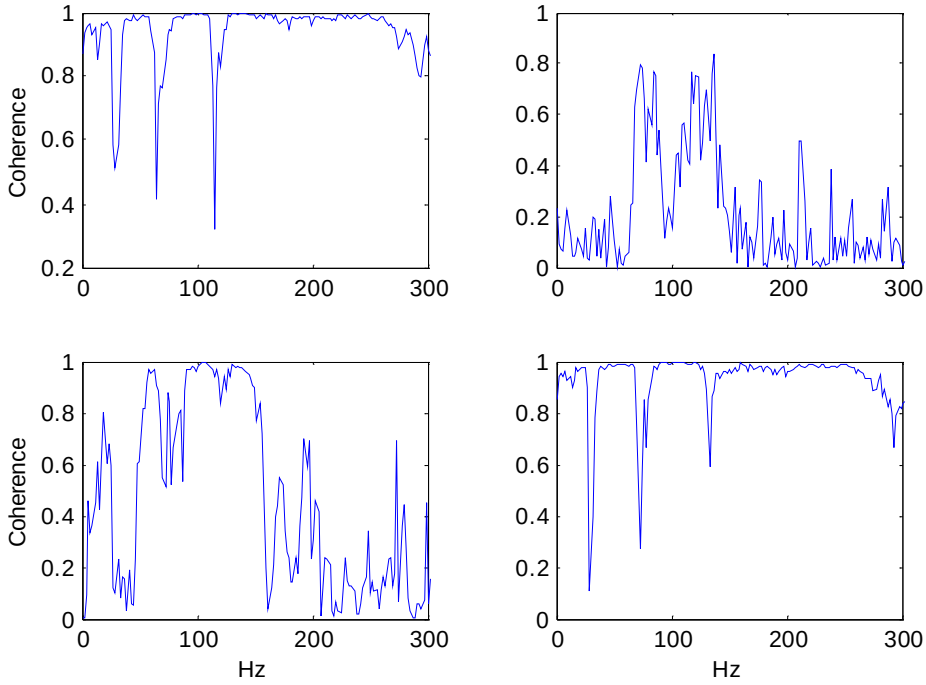

Figure 18: The coherence curves of the horizontal and vertical force frequency.

5 Comparison Between the Model and the Real System

In Figure 19 and Figure 20 are presented the vibration spectrums with different rotation speeds when the actuator cylinders are open and closed. The spectrums in Figure 19 are obtained with the simulation model and those in Figure 20 are measured from the real test bench. The cylinders open case is simulated by giving constant negative force set value of -1 kN to the PID force controller of each cylinder. In the cylinder closed case the set value has been +1 kN.

The following observations can be made:

- The simulated system has more unbalance, the first harmonic component rises exponentially when the rotation speed increases. In the real case the first harmonic component is nearly constant in this speed range.
- The constant value of the first harmonic component in the real case comes from the out of roundness of the roller surface, which effects the vibration measurement using laser distance sensors. In the simulated case out of roundness does not affect the vibration measurement.
- The second harmonic component has much higher peak in the real case when the cylinders are open, hence the different scales in displacement.
- The closing of the cylinders attenuates strongly the second harmonic component in the simulated case. In the real case no attenuation can be observed.
- In both simulated and real case the half critical speeds increases when the cylinders are closed. The exact half critical speeds are different but in the same area.

- In the real case the third harmonic is clearly visible. In the simulated case the higher harmonics are actually present but they are very small and invisible in the used scale.

The most notable difference is the attenuation of the second harmonic component in the simulated case when the cylinders are closed. It seems, that the tuning of the force feedback PID controllers has a significant effect on this. Some tests considering this are presented in Appendix C.

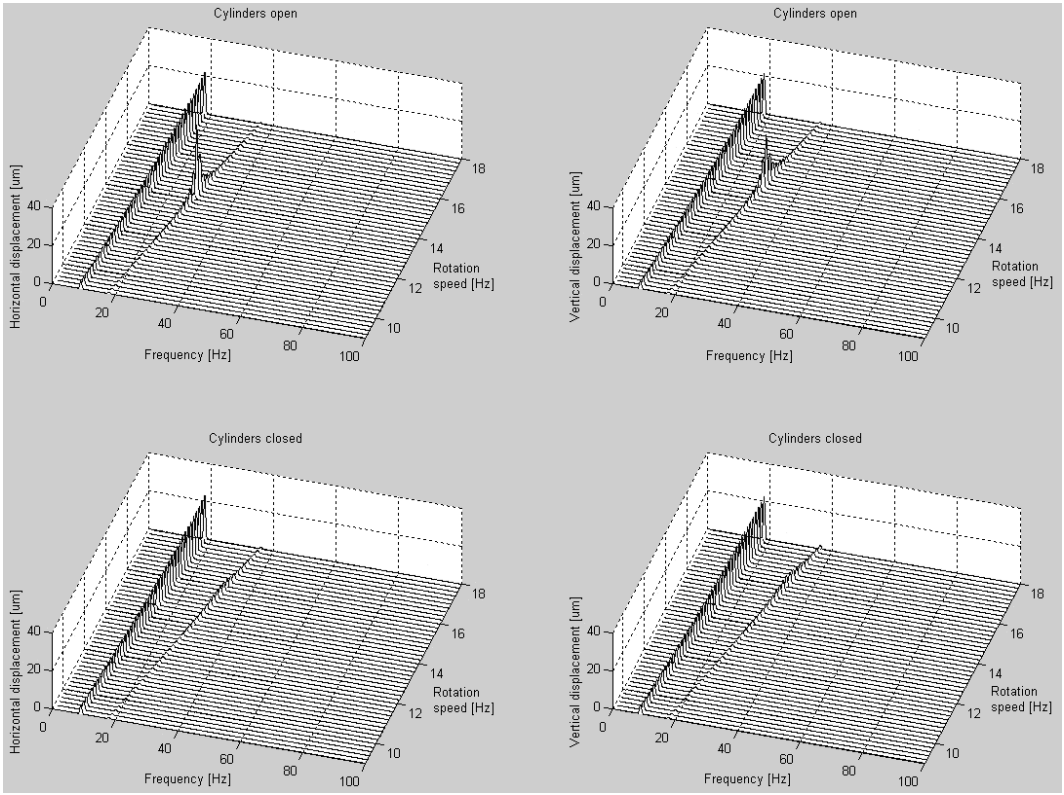

Figure 19: Simulated vibration spectrums at rotation speeds around the half critical speed.

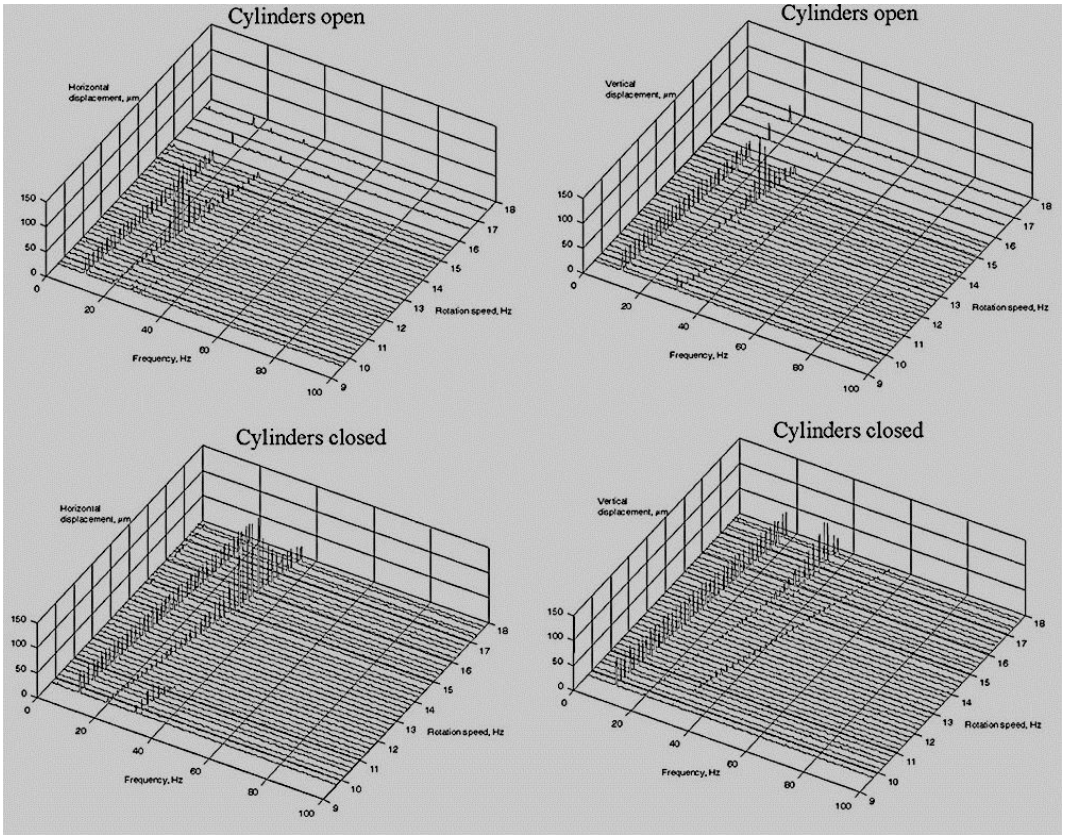

Figure 20: Measured vibration spectrums at rotation speeds around the half critical speed.

6 Frequency Response of the Damping System

The active damping algorithms need the frequency response between the actuator control, i.e. the set values for the horizontal and vertical forces, and the displacement measurements, horizontal and vertical, at the middle (length wise) of the roller. The control algorithms need the response at the frequencies corresponding the rotation speed and its first few multiples. In our case it is assumed, that the rotation speed does not significantly affect this response and, hence, the response can be measured using some low speed only. This is reasonable since the roller is a tube, which does not generate significant gyroscopic forces.

The frequency responses in horizontal and vertical directions were measured using noise control separately in both directions while the other direction had a constant force control value of 0 kN. The noise signal was the same as in Section 4.1 (see Figure 10). The results are presented in Figure 21 (gain) and Figure 22 (phase). The cross couplings are insignificantly small. The highest peaks in the diagonal gain curves are at about 30.5 Hz in the horizontal control case and at about 32.5 Hz in the vertical control case. The phase in the horizontal control case starts at +180 degrees, which means, that the measurement direction is negative. The coherence curves of the noise test are presented in Figure 23.

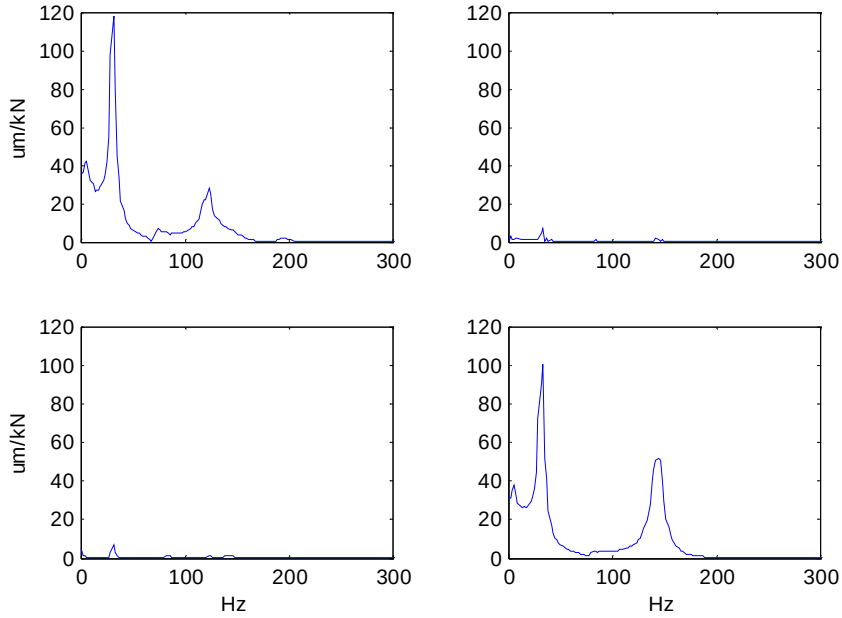

Figure 21: The gain curves of the frequency response between horizontal and vertical force set value signals and the corresponding displacements at the middle (length wise) of the roller. Horizontal force is controlled at the top row and vertical force at the bottom row. Horizontal displacements are at left and vertical displacements at right. The units are micrometer/kN. The rotation speed is 1 Hz.

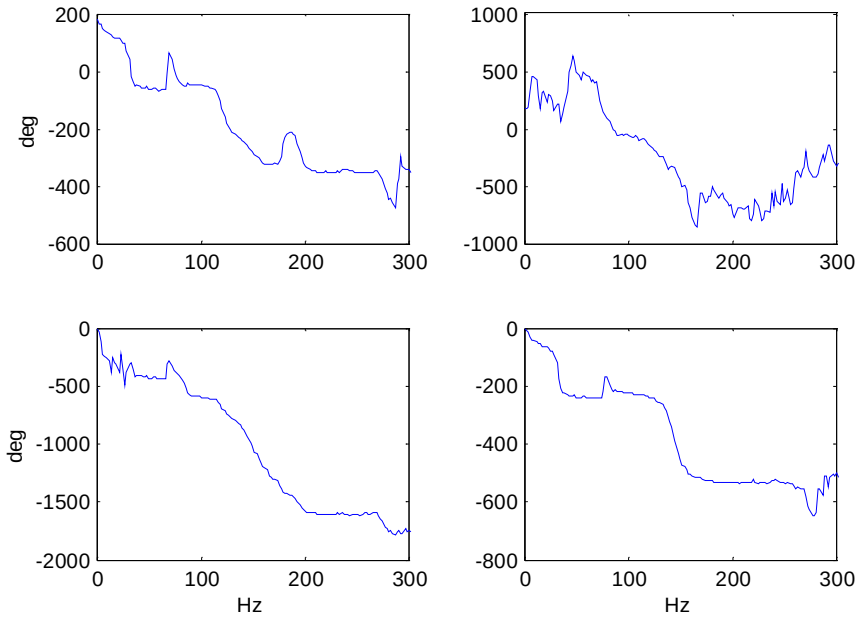

Figure 22: Phase curves of the frequency response of the displacement control.

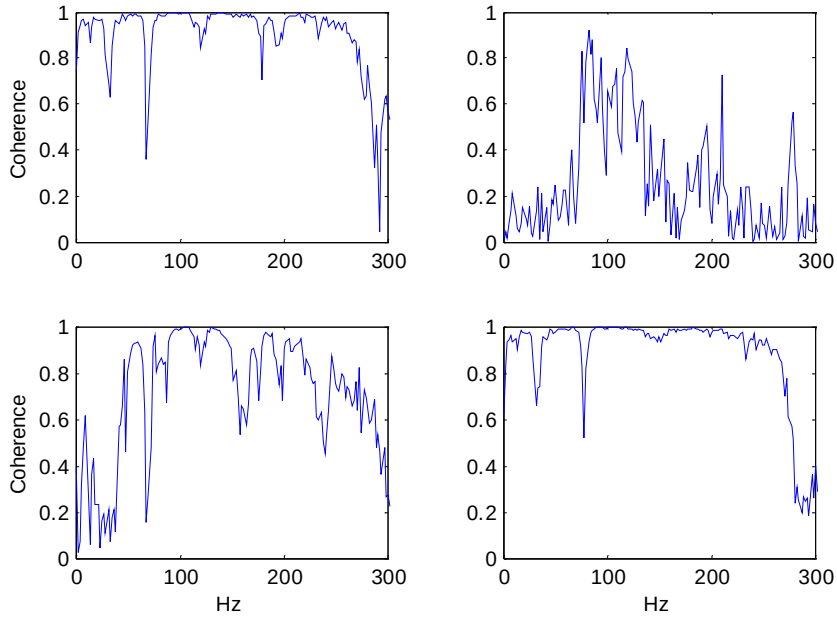

Figure 23: Coherence curves of the noise test of displacement control.

In order to be able to compute the frequency response value at any rotation speed a transfer function model is fitted to the measured responses. In Figure 24 and Figure 25 are shown the results of a weighted least squares estimation. The fitting was done only up to 100 Hz and only for the diagonal elements (cross couplings are regarded as negligible).

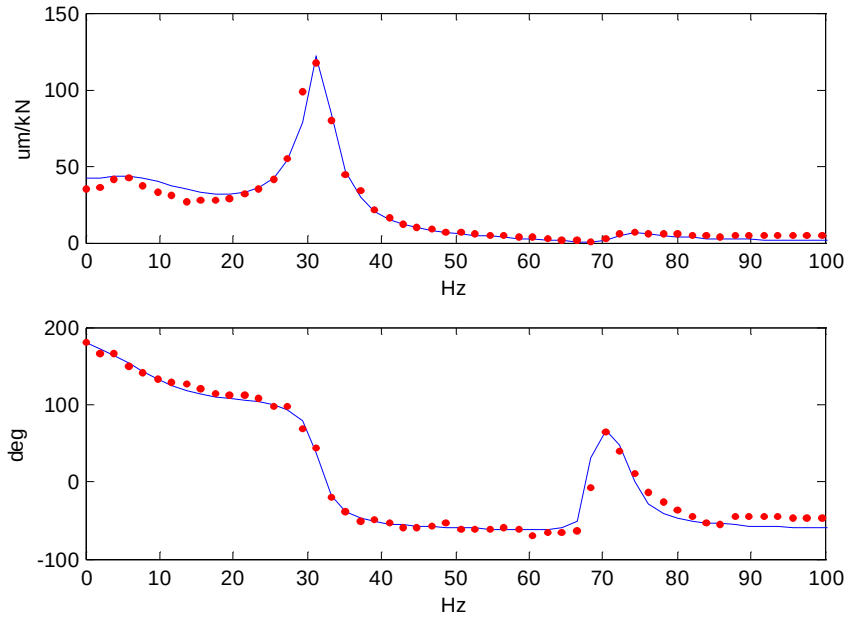

Figure 24: Frequency response (gain above and phase below) of the control of the horizontal displacement with the horizontal force. The red dots are obtained from the noise test and the blue line is from the fitted transfer function. (For later reference the fitting parameters for two stage fitting are: na1=2, nb1=1, maxfreq1=10, na2=4, nb2=3, maxfreq2=80, window = 4, Ts = 0.0005, tiedosto = 'xx.dat'.)

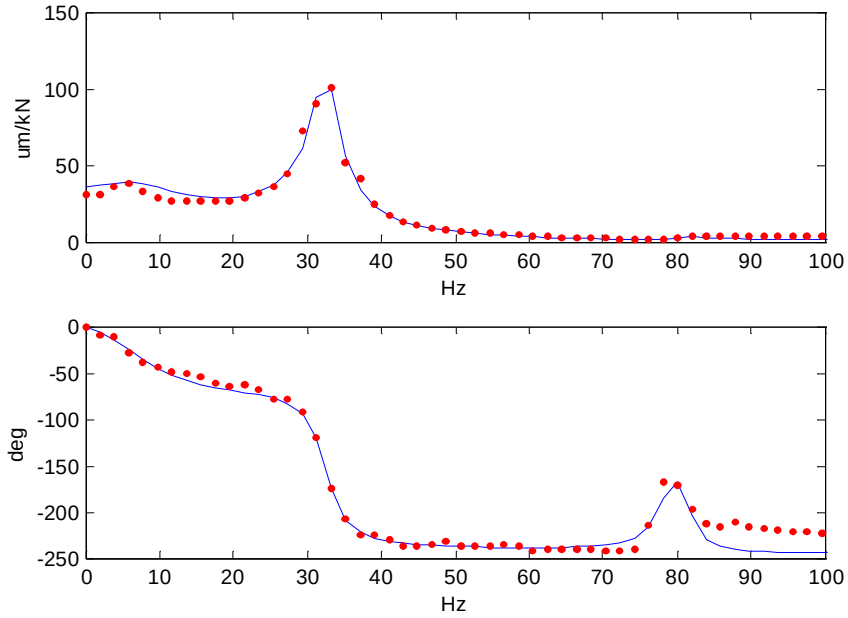

Figure 25: Frequency response (gain above and phase below) of the control of the vertical displacement with the vertical force. The red dots are obtained from the noise test and the blue line is from the fitted transfer function. (For later reference the fitting parameters for two stage fitting are: na1=2, nb1=1, maxfreq1=10, na2=4, nb2=3, maxfreq2=85, window = 4, Ts = 0.0005, tiedosto = 'yy.dat').

The transfer functions are:

- Horizontal control

$$G_{xx}(s)=\frac{504.0(s-658.6)(s+262.5)(s+91.04)(s^2+9.797s+427.5^2)}{(s^2+96.12+63.75^2)(s^2+21.09s+199.0^2)(s^2+26.80s+461.3^2)} \quad (3)$$

- Vertical control

$$G_{yy}(s)=\frac{-368.7(s-728.7)(s+341.4)(s+59.09)(s^2+26.75s+492.0^2)}{(s^2+88.05s+57.53^2)(s^2+22.73s+204.5^2)(s^2+22.11s+511.0^2)} \quad (4)$$

The nominal frequencies of these models with corresponding damping ratios are shown in Table 6.

Table 6: Nominal frequencies and damping ratios of the transfer functions.

Horizontal control		**Vertical control**	
Frequency, Hz	Damping ratio	Frequency, Hz	Damping ratio
10.1	0.754	9.2	0.765
31.7	0.053	32.5	0.056
73.4	0.029	81.3	0.022

7 Active Damping Tests

7.1 Higher Harmonic Control

The principle of Higher Harmonic Control (HHC) for damping one frequency in shown in Figure 26 [Järviluoma 2003], taken from [Hall & Wereley 1989]. The principle involves the computation of the Fourier coefficient of the disturbance at the damped frequency and setting the Fourier coefficients of the control signal so, that the disturbance is cancelled at this frequency. In our case the plant $P(s)$ includes the roller and the force actuator system with the PID force feedback controls. The input signal $u(t)$ is either the horizontal or vertical set value for the force controller. The measured vibration $y(t)$ is either the horizontal or vertical displacement measured from the centre (length wise) of the roller. The transfer functions used for computing the a and b are the ones defined in the previous section.

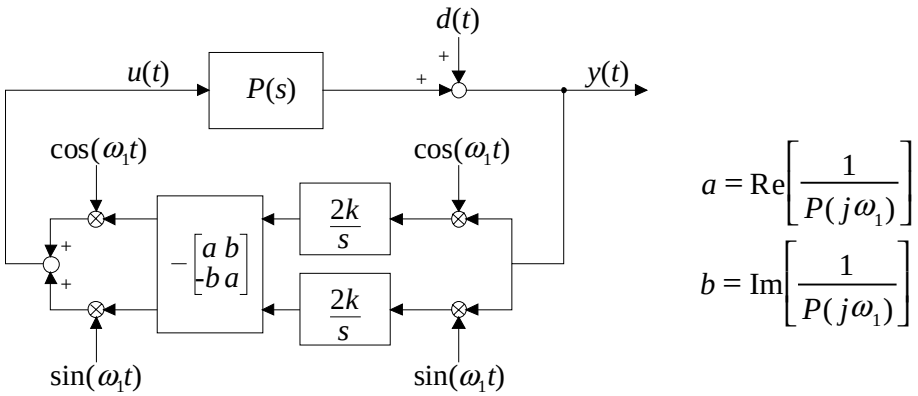

Figure 26: Higher Harmonic Control (HHC) principle. P(s) is the transfer function of the controlled system and d is the disturbance, y is the measured vibration and u is the control signal. The disturbance frequency ω_1 is to be attenuated.

In our case the algorithm is used in a discrete time form.

$$u(kh) = \theta_1(kh)\cos(k\omega_1 h) + \theta_2(kh)\sin(k\omega_1 h) \tag{5}$$

$$\begin{bmatrix}\theta_1(kh+h)\\ \theta_2(kh+h)\end{bmatrix} = \begin{bmatrix}\theta_1(kh)\\ \theta_2(kh)\end{bmatrix} - Ky(kh)\begin{bmatrix}R(\omega_1) & -I(\omega_1)\\ I(\omega_1) & R(\omega_1)\end{bmatrix}\begin{bmatrix}\cos(k\omega_1 h)\\ \sin(k\omega_1 h)\end{bmatrix}\frac{1}{R(\omega_1)^2 + I(\omega_1)^2} \tag{6}$$

where h is the sample interval (1 ms) and $R(\omega_1)$ and $I(\omega_1)$ are the real and imaginary parts of the frequency response $P(j\omega_1)$. It can be shown, that this control corresponds to constant parameter feedback control with controller transfer function

$$\frac{U(z)}{Y(z)} = -K\frac{1}{A(\omega_1)}\frac{\cos(\omega_1 h - \phi(\omega_1)) - \cos(\phi(\omega_1))}{z^2 - 2\cos(\omega_1 h)z + 1} \tag{7}$$

where $A(\omega_1)$ is the gain and $\phi(\omega_1)$ is the phase of $P(j\omega_1)$. The controller has complex undamped poles at the unit circle corresponding the attenuated frequency and it cancels the system gain at that frequency.

In the simulation tests the damped frequency was either the rotation speed of the roller or its double. Also simultaneous damping of both was simulated. In that case the HHC algorithms were duplicated and their outputs added together. In all simulations both the horizontal and vertical vibrations were damped simultaneously.

As a practical addition it was noted, that the possible non-zero dc-level of the displacement measurements must be filtered out with a high pass filter $(z\text{-}1)/(z\text{-}0.9995)$ before feeding them to the damping algorithm. Otherwise some dc forces are generated, which tend to bend the roller and alter its dynamics.

In Figure 27 is shown the displacements in the two directions when the damping of the first and second harmonic component is started at the instant 5000 ms. The roller is rotating at 16 Hz speed, which is close to the half critical speeds (which are slightly different in different directions). The damping gain (or adaptation gain) K is 0.01 (displacements in micrometers, control outputs in kN). The convergence is good.

In Figure 28 and Figure 29 are presented the spectrums of horizontal and vertical displacements from the following test runs at speed 16 Hz.

- Undamped run: the 1st and 2nd harmonic components are dominating in both directions.
- 1st harmonic damping: works well, the 2nd and 3rd harmonics rise a bit.
- 2nd harmonic damping: works well, doesn't remove the 2nd harmonic completely though, higher harmonics do not rise.
- 1st and 2nd harmonic damping: works well, doesn't remove the 2nd harmonic completely though, the 3rd harmonic rises a bit.

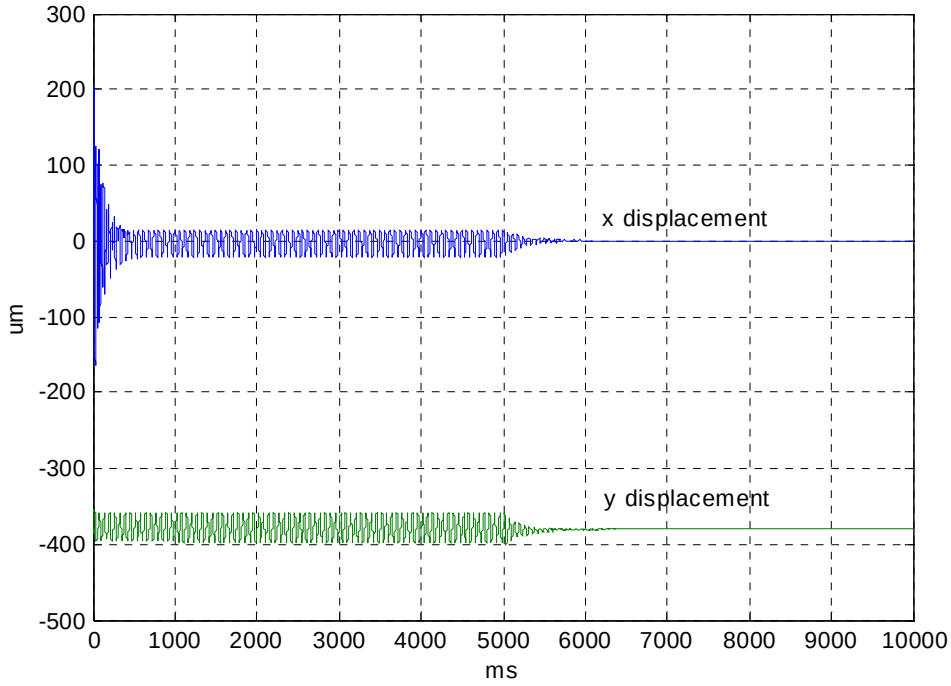

Figure 27: HHC damping at the 1st and 2nd harmonic frequency (gain 0.01) in x- and y-directions, starting at 5000 ms. The rotation speed is 16 Hz.

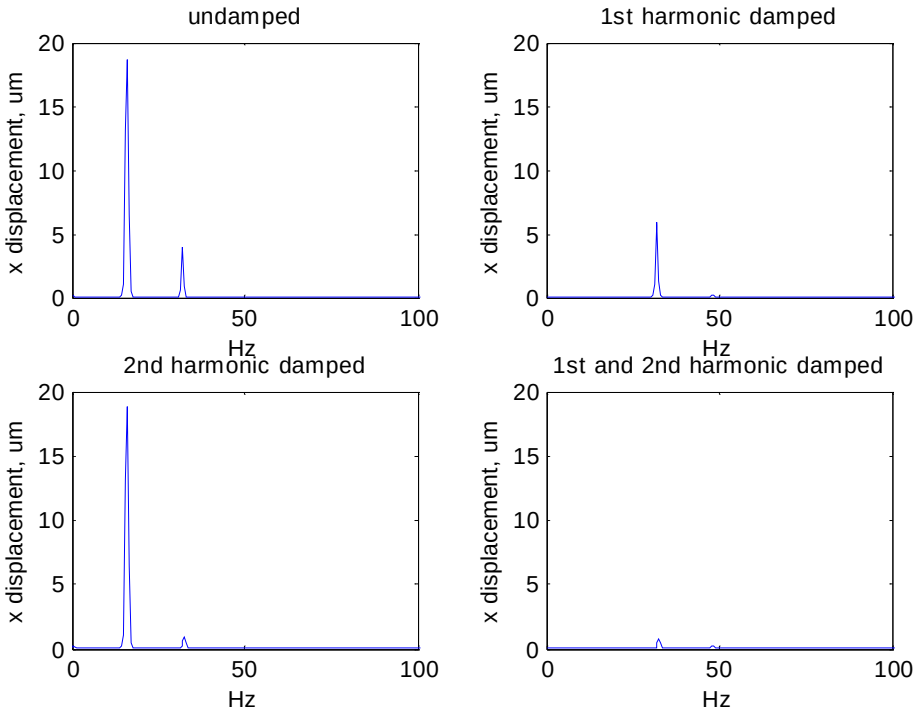

Figure 28: The spectrums of the horizontal displacements in four cases. Damped with HHC algorithms with gain 0.01. Rotation speed is 16 Hz.

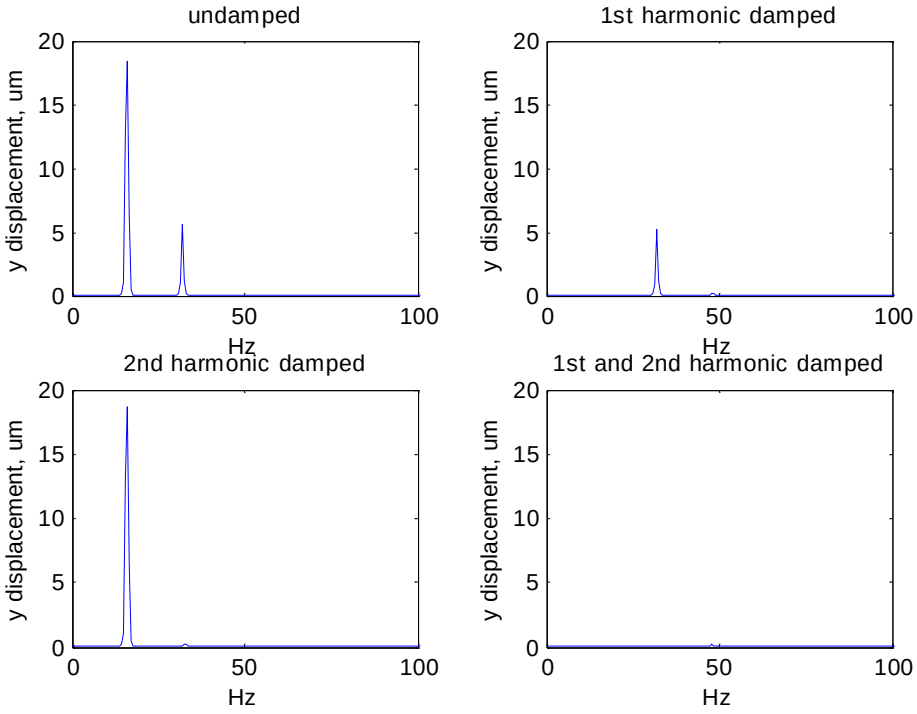

Figure 29: The spectrums of the vertical displacements in four cases. Damped with HHC algorithms with gain 0.01. Rotation speed is 16 Hz.

In Figure 30 and Figure 31 are presented the displacements from damping tests at rotation speed 32 Hz, which is near the critical speeds. The spectrums of the horizontal and vertical displacements are presented in Figure 32 an Figure 33. It can be noted, that the damping of the 1st harmonic works well but the damping of the 2nd harmonic is unstable. The gain of the

damping algorithm is 0.01, i.e. the same as was used with lower speed. The damping of the second harmonic component, i.e. 64 Hz, would have required lower gain.

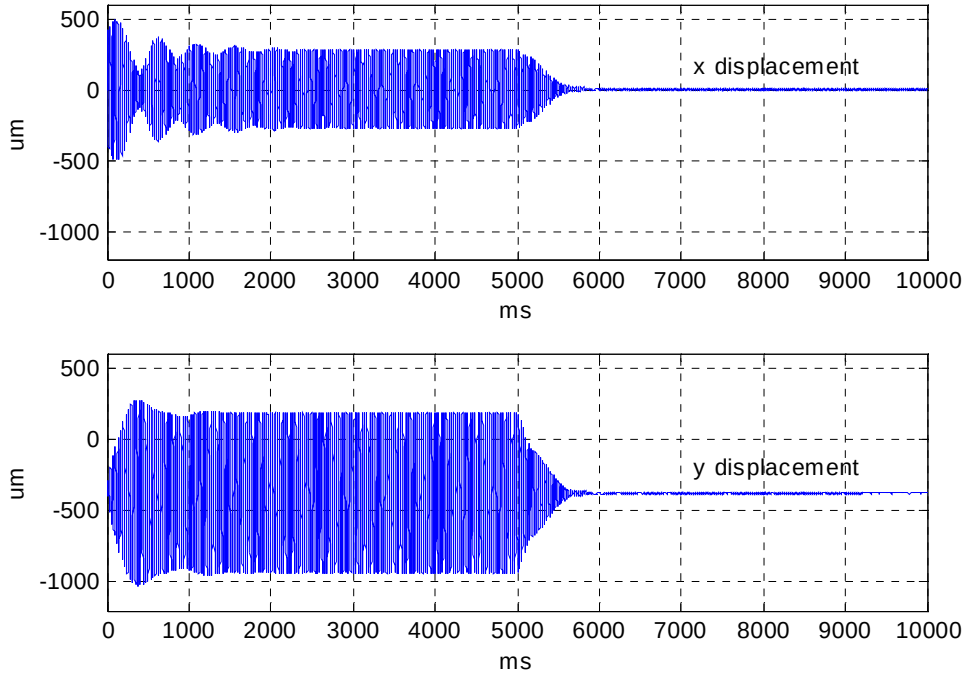

Figure 30: The damping of the 1st harmonic at rotation speed 32 Hz. HHC damping with gain 0.01, starting at 5000 ms.

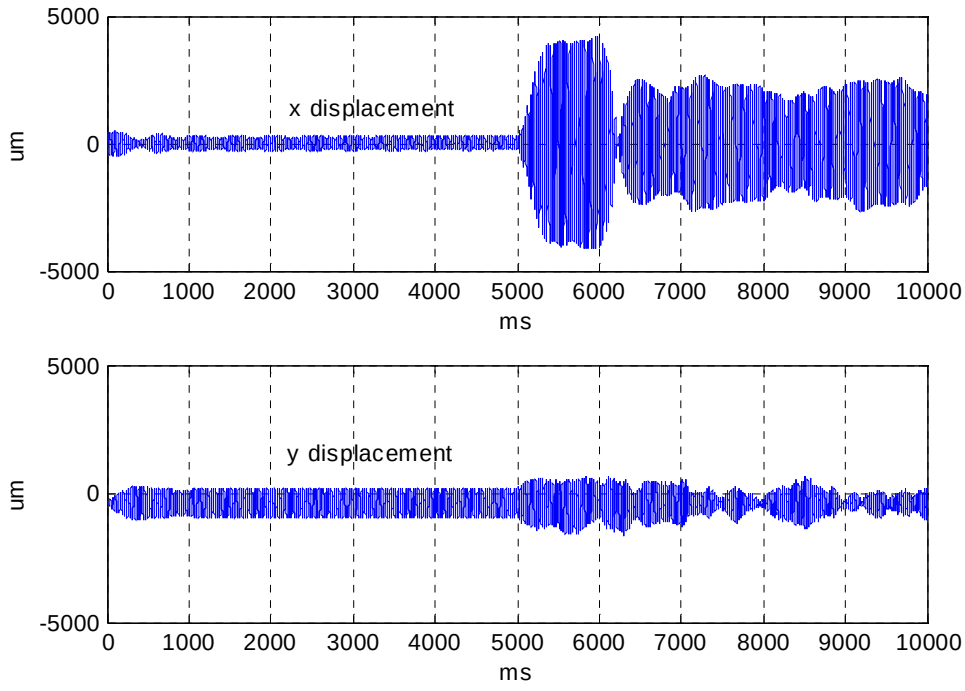

Figure 31: The damping of the 1st and 2nd harmonic at speed 32 Hz. HHC damping with gain 0.01, starting at 5000 ms. Control becomes unstable.

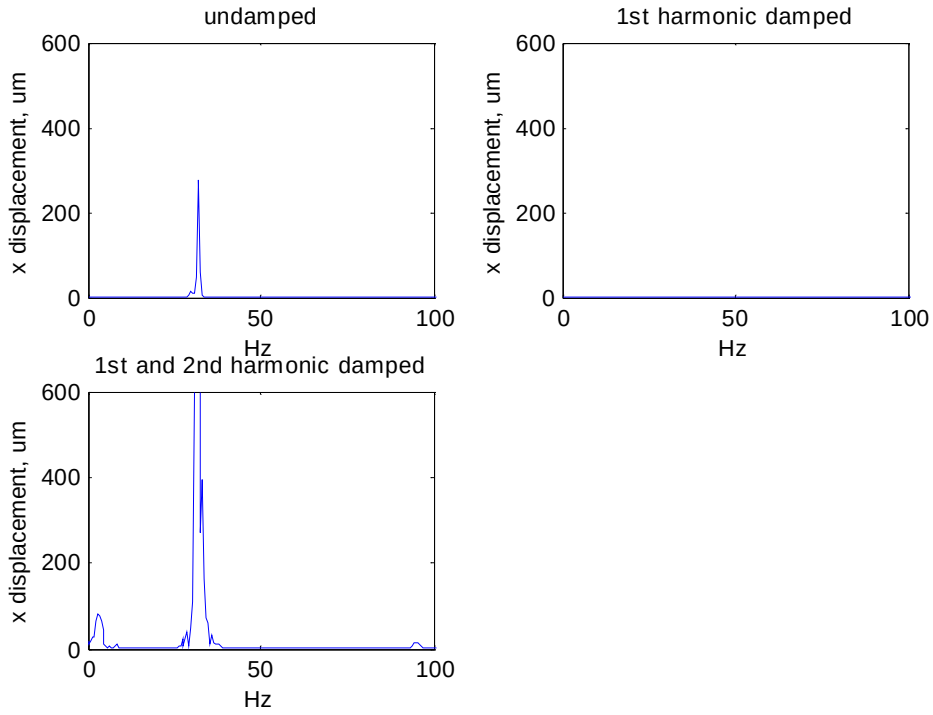

Figure 32: The spectrums of the horizontal displacements at three cases with rotation speed 32 Hz. The 1st and 2nd harmonic damping case (at bottom row) is unstable.

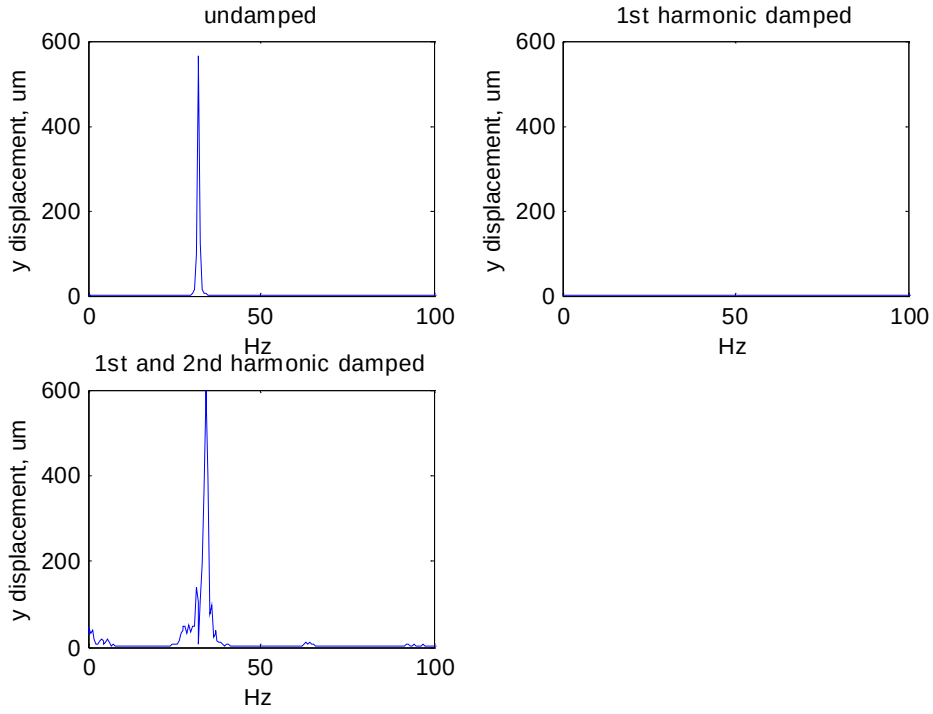

Figure 33: The spectrums of the vertical displacements at three cases with rotation speed 32 Hz. The 1st and 2nd harmonic damping case (at bottom row) is unstable.

The active damping was also tested with accelerating rotation. In Figure 34 and Figure 35 are presented the case, where the roller is accelerated over the critical speeds with and without active damping. The acceleration has been rather high, 0.5 Hz/s. In this case the damping algorithm works well.

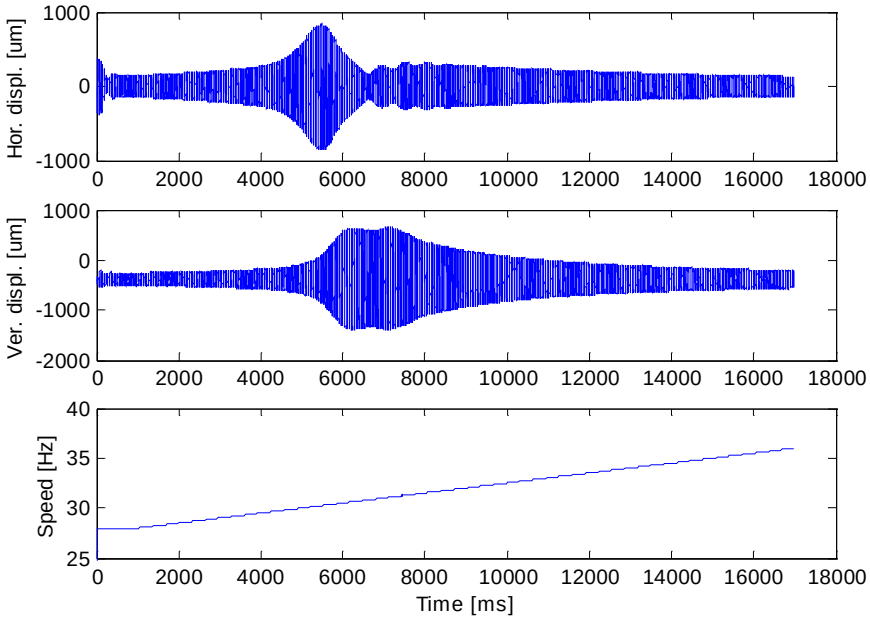

Figure 34: Accelerating beyond the critical speeds with 0.5 Hz/s. No active damping. Constant force set values 1 kN.

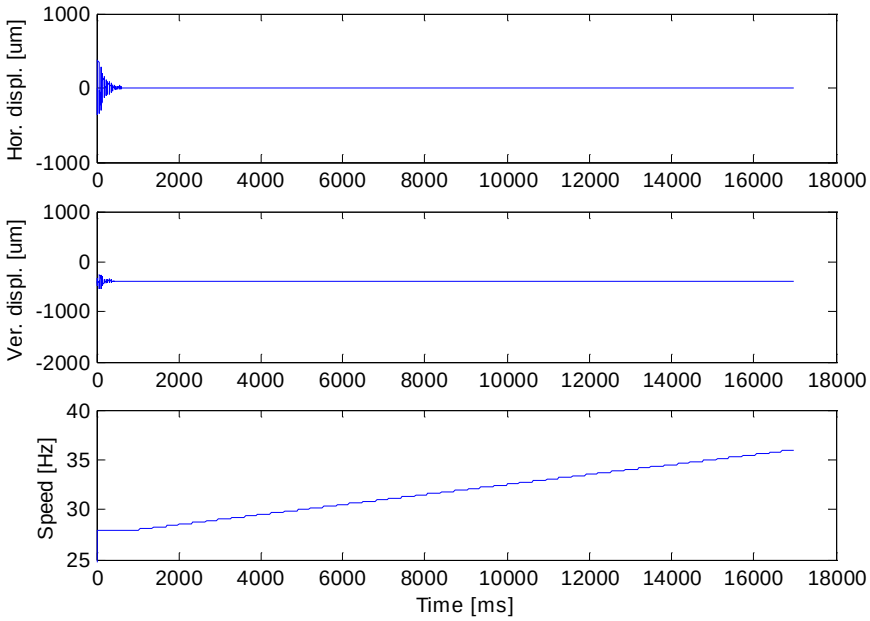

Figure 35: Accelerating beyond the critical speeds with 0.5 Hz/s. First harmonic HHC damping with gain 0.01.

7.2 Convergent Control

The active damping principle, which was used in the tests carried out in PYÖRIVÄRE project was called convergent control. It was adapted from [Knospe et al. 1995, Burrows et al. 1989] and is described in [Järviluoma & Valkonen 2002]. The method is based on computing the Fourier coefficients of the vibration signals at the damped frequencies (rotation speed or its multiples) over a time interval of one or more base periods of the vibration. The Fourier

coefficients of the control signals (force set values in this case) are then computed according to these and the known frequency response of the damping system as

$$\overline{U}_{k+1} = \overline{U}_k - \overline{T}^{-1}\overline{D}_{k+1} \tag{8}$$

where vector $\overline{U}_k$ includes the complex Fourier coefficients of the control signals (horizontal and vertical) at update instant *k*, $\overline{D}_k$ contains the complex Fourier coefficients of the displacement signals (horizontal and vertical) and $\overline{T}$ is the 2x2 frequency response matrix at the considered frequency.

Exactly the same control algorithm was tested also with the simulation model. An example of the damping of the first harmonic frequency is shown in Figure 36 and Figure 37 (the CC parameters are: number of periods in Fourier coefficient calculations is 2, settling delay before next update cycle is 0.2 seconds, Fourier coefficients of the control signals are updated using a ramp function of duration equal to 2 periods of vibration). When compared to HHC damping, the convergent control behaves much worse. The simultaneous damping of the 1st and 2nd harmonic frequencies did not work at all with the actual test bench in PYÖRIVÄRE project. The failure of the convergent control is apparent also in the simulation, the results of which are shown in Figure 38 and Figure 39. The reason for this is under investigation, the following are the current hypotheses:

- The damping of the 1st harmonic component creates a constant force, which is rotating with the roller and is causing a constant bending strain in it. This changes the frequency response of the damping system to some extent. The HHC damping algorithm is more robust to this change than the convergent control.
- The hydraulic actuator system is non-linear and it creates higher harmonic components. The generation of forces at the 1st harmonic frequency causes disturbances at the 2nd harmonic frequency, which then disturb the damping at that frequency. Again, the HHC damping seems to be more insensitive to this.
- Error in simulation.

In Appendix D are presented the results from a simplified test with both CC and HHC algorithms, where the ADAMS model was replaced with linear transfer functions. The CC and HHC algorithms were exactly the same (same C functions) as the ones used with the ADAMS model and the transfer function models were the same that are used in the control algorithms. The results show, that the algorithms are working properly. Hence, it can be assumed, that the problems are caused by the non-linear dynamics of the roller and actuators.

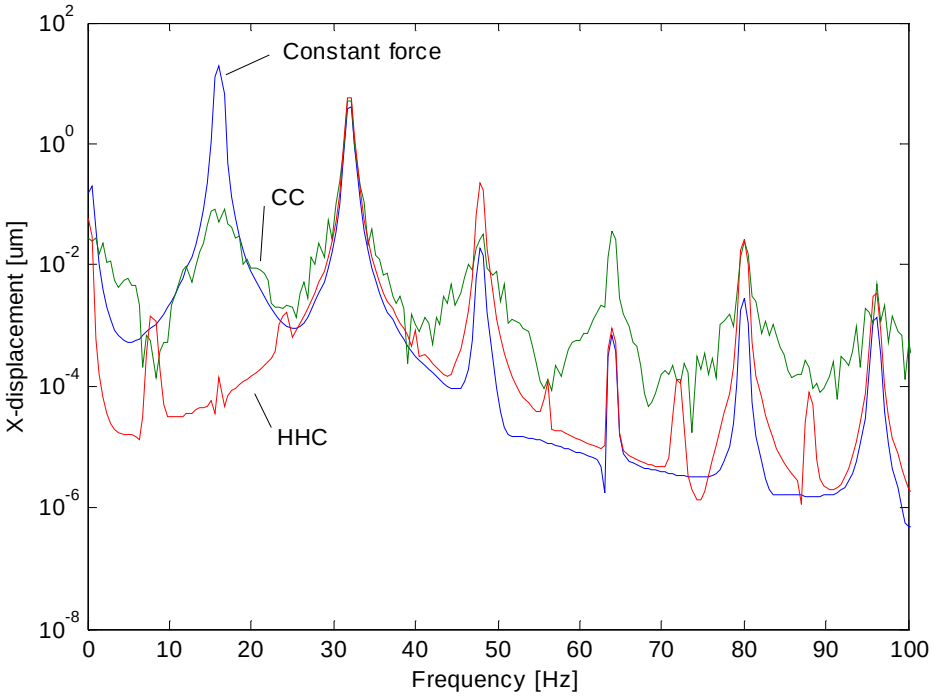

Figure 36: Damping the 1st harmonic frequency at speed 16 Hz, the spectrums of the horizontal displacements in three cases: without active damping ('Constant force', blue line), with HHC damping ('HHC', red line) and with convergent control ('CC', green line).

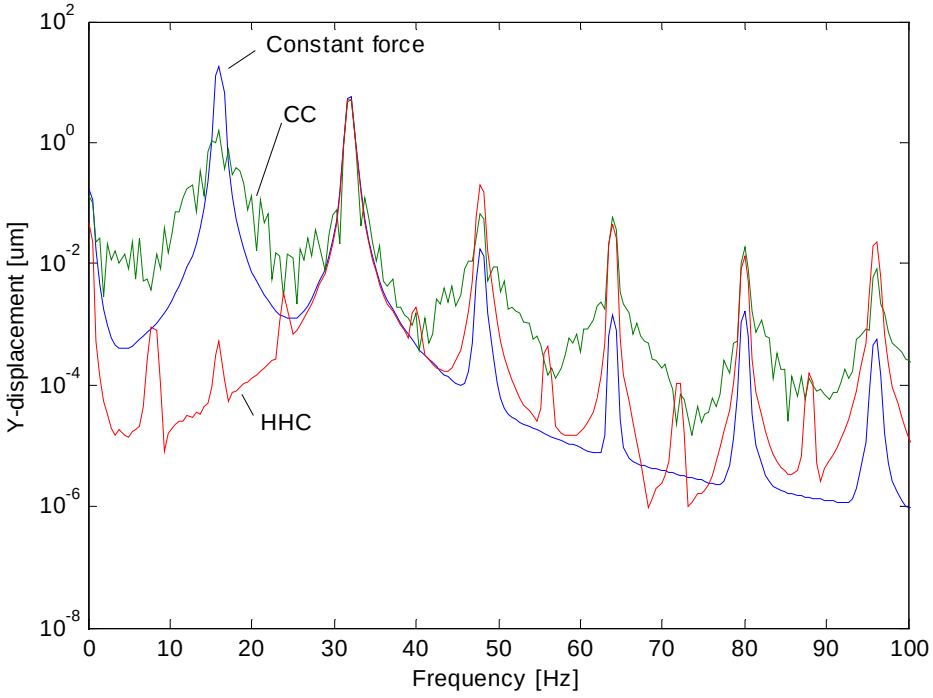

Figure 37: Damping the 1st harmonic frequency at speed 16 Hz, the spectrums of the vertical displacements in three cases: without active damping ('Constant force', blue line), with HHC damping ('HHC', red line) and with convergent control ('CC', green line).

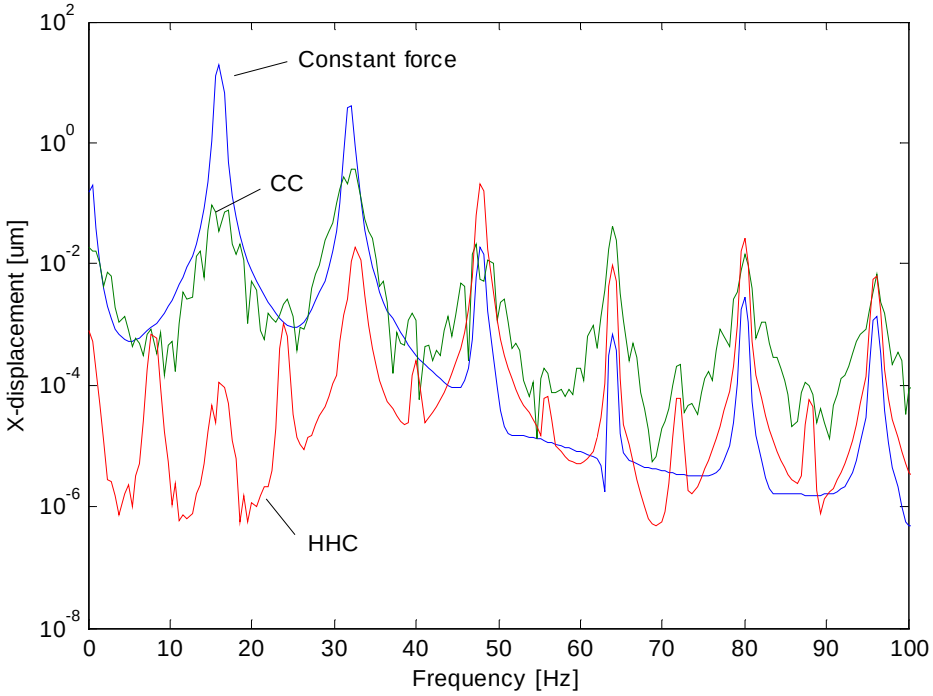

Figure 38: Damping the 1st and 2nd harmonic frequencies at speed 16 Hz, the spectrums of the horizontal displacements in three cases: without active damping ('Constant force', blue line), with HHC damping ('HHC', red line) and with convergent control ('CC', green line).

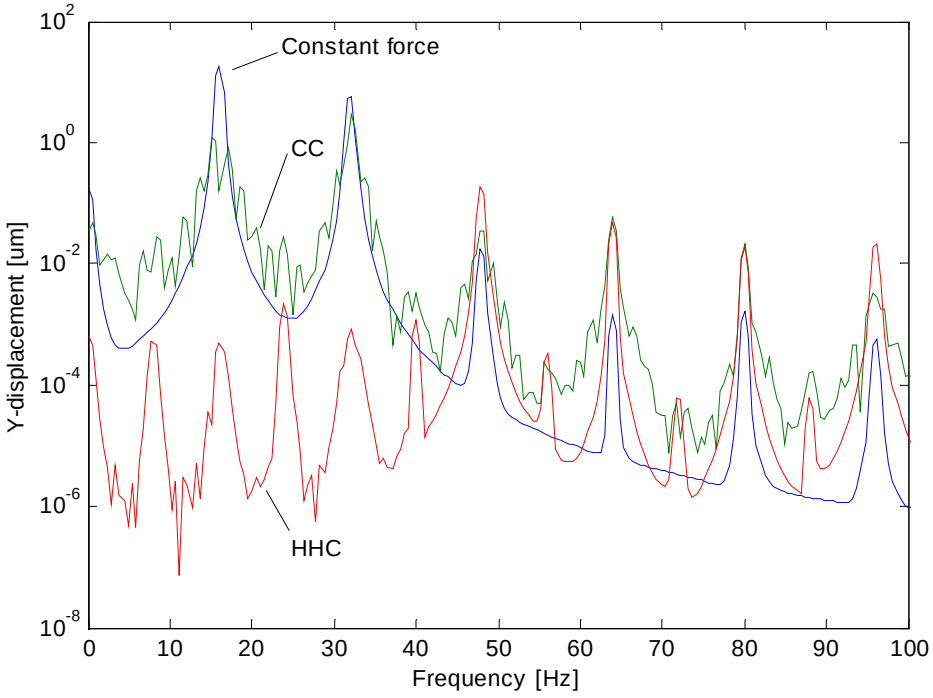

Figure 39: Damping the 1st and 2nd harmonic frequencies at speed 16 Hz, the spectrums of the vertical displacements in three cases: without active damping ('Constant force', blue line), with HHC damping ('HHC', red line) and with convergent control ('CC', green line).

8 Conclusions

The ADMAS model of the mechanical system and hydraulics is working reasonably fast with discrete time simulation with 0.5 ms communication interval. Also the interface between the Simulink model of the control system and the ADAMS model seems to work without problems.

The behaviour of the model does simulate reality within reasonable limits. The observed major differences can be explained by differences in rotor balance and in the tuning of the force feedback control.

The frequency response between the force actuators and the vibration of the roller was measured and modelled only with one rotation speed (1 Hz). It seems, that in this case this was enough, the response does not change significantly with higher rotation speeds.

The HHC damping algorithm works well both with single frequencies and with multiple harmonics. The gain of the controller can be the same for frequencies above the critical speed but must be decreased if frequencies of about twice the critical speed or above that are damped. Hence, the tuning of the HHC is relatively simple, provided that an accurate enough frequency response information at the damped frequencies is available.

The convergent control method, which was used also in the tests with the real device, turned out to behave much worse than HHC damping. It also showed in simulation the same kind of problems as it did in real tests in the damping of the 1st and 2nd harmonics near the half critical speed.

References

Järviluoma M., Valkonen A., *Test equipment and controller for active rotor vibration damping: set-up, methods and test results*, Progress report 2, PYÖRIVÄRE / Rotor Vibration Control, Oulu, 28.2.2002, Finland.

Sopanen J., *PyöriVÄRE-project: ADAMS Simulation Model of the Roller Test Rig, Balancing Machine Support*, Lappeenranta, 17.5.2002, Finland.

Kemppainen R., *Aktiivinen värähtelynhallintalaite*, 020840000 Virtuaalisuunnittelun erikoistyö, Lappeenranta, 14,6,2001, Finland.

Hall, S.R., Wereley, N.M., *1989. Linear control issues in the higher control of helicopter vibrations*. Proc. 45th Annu. Forum Amer. Helicopter Soc. (Boston, MA), May 1989. Pp. 955-971.

Knospe, C.R. & Hope, R.W. & Fedigan S.J. & Williams, R.D., 1995. *Experiments in the control of unbalance response using magnetic bearings*. Mechatronics, vol. 5, no. 4, pp. 385-400.

Burrows, C.R. & Sahinkaya, M.N. & Clements, S., 1989. *Active vibration control of flexible rotors: an experimental and theoretical study*. Proceedings of the Royal Society of London, vol. A 422, pp. 123-146.

Appendix A: Mass Properties of the Model Parts

Mass properties of the flexible and rigid parts are shown in Table 1 and Table 2. In Table 1 there are three massless parts (dummy_akt, dummy_hp and dummy_kp). These parts are used to make point-to-curve connections between flexible and rigid parts. These massless parts don't have any influence to the simulation of the model.

Table 1: Mass properties of the flexible parts.

Part	Mass [kg]	Ixx [kgm^2]	Iyy [kgm^2]	Izz [kgm^2]	Ixy [kgm^2]	Iyz [kgm^2]	Izy [kgm^2]
tela	756,0	6,382E+03	6,382E+03	1,382E+01	5,084E-03	-7,160E-03	-6,779E-02
vaimennin	841,7	1,887E+02	1,618E+02	2,940E+02	0,000E+00	0,000E+00	0,000E+00
ylaosa_kp	41,0	7,780E+00	5,754E+00	2,141E+00	1,002E-05	-8,076E-03	8,387E-06
ylaosa_hp	41,0	7,780E+00	5,754E+00	2,141E+00	1,002E-05	-8,076E-03	8,387E-06

Table 2: Mass properties of the rigid parts.

Part	Mass [kg]	Ixx [kgm^2]	Iyy [kgm^2]	Izz [kgm^2]
sylinteri_1	8,1	1,568E-02	9,618E-02	9,618E-02
varsi_1	8,8	3,891E-03	1,377E-01	1,377E-01
sylinteri_2	8,1	1,568E-02	9,618E-02	9,618E-02
varsi_2	8,8	3,891E-03	1,377E-01	1,377E-01
sylinteri_3	8,1	1,568E-02	9,618E-02	9,618E-02
varsi_3	8,8	3,891E-03	1,377E-01	1,377E-01
laakeripesa_akt	46,4	9,680E-01	4,949E-01	4,949E-01
holkki_1	4,4	8,487E-03	8,360E-03	4,003E-03
holkki_2	4,4	8,487E-03	8,360E-03	4,003E-03
holkki_3	4,4	8,487E-03	8,360E-03	4,003E-03
dummy_akt	(none)	-	-	-
dummy_hp	(none)	-	-	-
dummy_kp	(none)	-	-	-
alalevy_kp	19,6	4,508E-01	2,101E-02	4,635E-01
alalevy_hp	19,6	4,508E-01	2,101E-02	4,635E-01
laakeripesa_kp	65,9	7,840E-01	1,477E+00	8,780E-01
laakeripesa_hp	65,9	7,840E-01	1,477E+00	8,780E-01

Appendix B: Model Damped Natural Frequencies

Table 1: Damped natural frequencies and damping ratios of the simulation model.

Mode	Frequency [Hz]	Damping Ratio	Mode	Frequency [Hz]	Damping Ratio	Mode	Frequency [Hz]	Damping Ratio
24	28,5	0,4 %	56	449,6	5,3 %	88	751,5	9,6 %
25	29,5	0,9 %	57	1995,3	97,4 %	89	755,2	10,3 %
26	65,3	0,5 %	58	460,0	9,8 %	90	777,2	10,0 %
27	72,8	1,4 %	59	482,6	8,5 %	91	786,2	9,9 %
28	83,6	1,3 %	60	1054,3	88,7 %	92	849,6	10,4 %
29	87,6	1,0 %	61	493,6	9,3 %	93	867,3	9,8 %
30	118,2	1,0 %	62	506,6	0,7 %	94	876,7	10,1 %
31	120,8	9,5 %	63	506,9	0,7 %	95	1801,4	87,1 %
32	123,6	3,9 %	64	1604,4	94,5 %	96	997,7	46,1 %
33	127,7	9,9 %	65	557,2	9,8 %	97	893,8	2,5 %
34	133,6	1,2 %	66	559,7	9,7 %	98	908,1	10,7 %
35	150,0	10,0 %	67	1604,4	93,8 %	99	916,9	9,8 %
36	150,0	10,0 %	68	592,8	9,5 %	100	1198,7	63,6 %
37	150,0	10,0 %	69	601,4	9,8 %	101	1195,2	62,8 %
38	158,7	1,9 %	70	616,9	9,8 %	102	1034,9	43,3 %
39	185,1	2,0 %	71	1027,6	78,9 %	103	1030,0	41,6 %
40	207,8	24,4 %	72	640,2	9,7 %	104	972,9	10,2 %
41	202,1	2,1 %	73	645,6	9,9 %	105	976,1	10,0 %
42	1048,2	98,0 %	74	1454,1	89,5 %	106	996,9	1,1 %
43	216,0	23,4 %	75	653,5	9,2 %	107	1007,1	0,8 %
44	218,4	24,1 %	76	661,1	10,0 %	108	1367,2	47,4 %
45	273,5	2,4 %	77	678,1	9,9 %	109	1206,3	2,0 %
46	281,7	2,0 %	78	694,7	10,0 %	110	1222,8	0,7 %
47	286,8	5,7 %	79	693,6	7,6 %	111	1264,7	22,4 %
48	332,8	9,6 %	80	700,4	7,5 %	112	1303,9	20,5 %
49	369,5	9,1 %	81	706,0	9,9 %	113	1413,3	0,7 %
50	375,1	4,6 %	82	709,4	9,9 %	114	1415,2	0,7 %
51	379,5	8,8 %	83	1495,4	88,1 %	115	1543,1	0,7 %
52	392,5	6,1 %	84	730,1	10,0 %	116	1544,4	0,7 %
53	395,9	8,9 %	85	738,7	9,9 %	117	1714,8	13,9 %
54	418,9	10,0 %	86	741,8	1,0 %	118	1717,0	14,0 %
55	422,5	10,0 %	87	747,1	0,9 %			

Appendix C: Effect of the Tuning of Force Feedback Controllers on the Vibration of the Roller

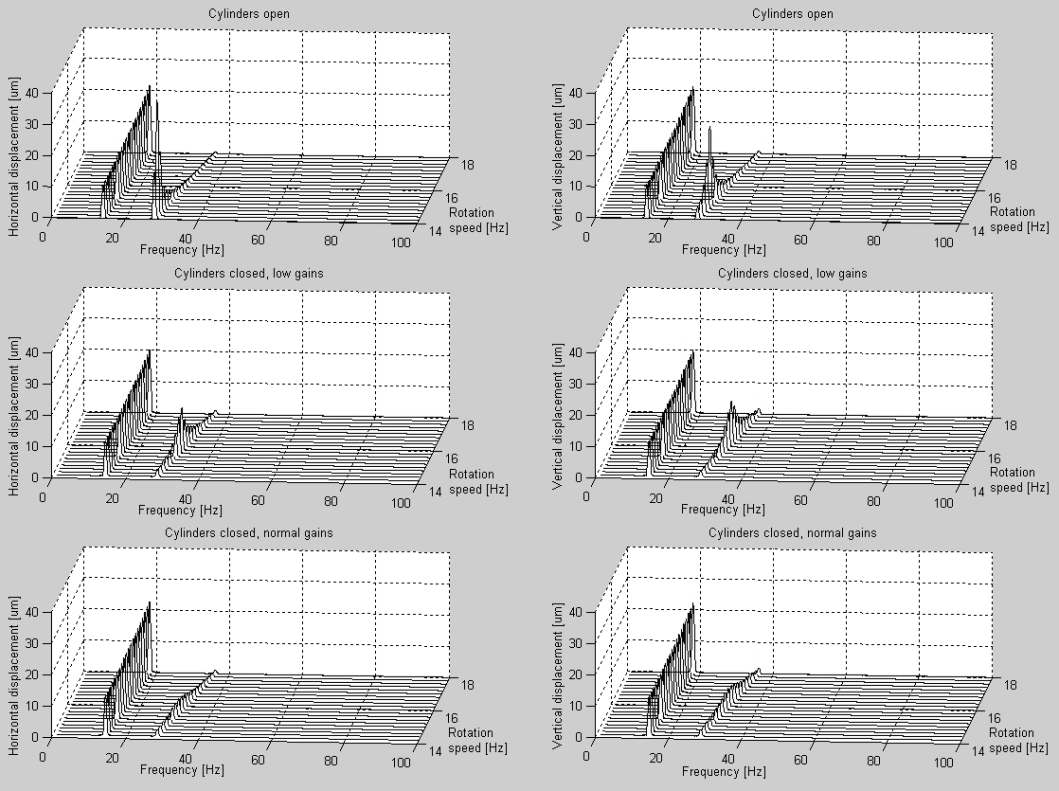

Figure 1: Vibration spectrums at the centre (length wise) of the roller when the cylinders are open (top row), when the cylinders are closed with low gains in force feedback PID controllers (middle row), and when the cylinders are closed with normal gains in force feedback PID controllers. Horizontal vibrations at left column and vertical vibrations in right column. The force feedback controllers have had constant set values of -1 kN (cylinder open case) or +1 kN (cylinders closed case).

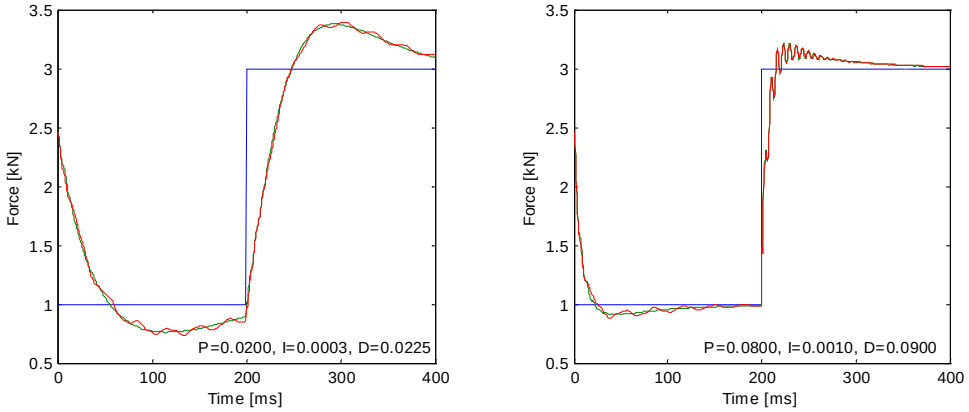

Figure 2: Cylinder force step responses with low gain force feedback PID-control (left) and normal gain PID-control (right).

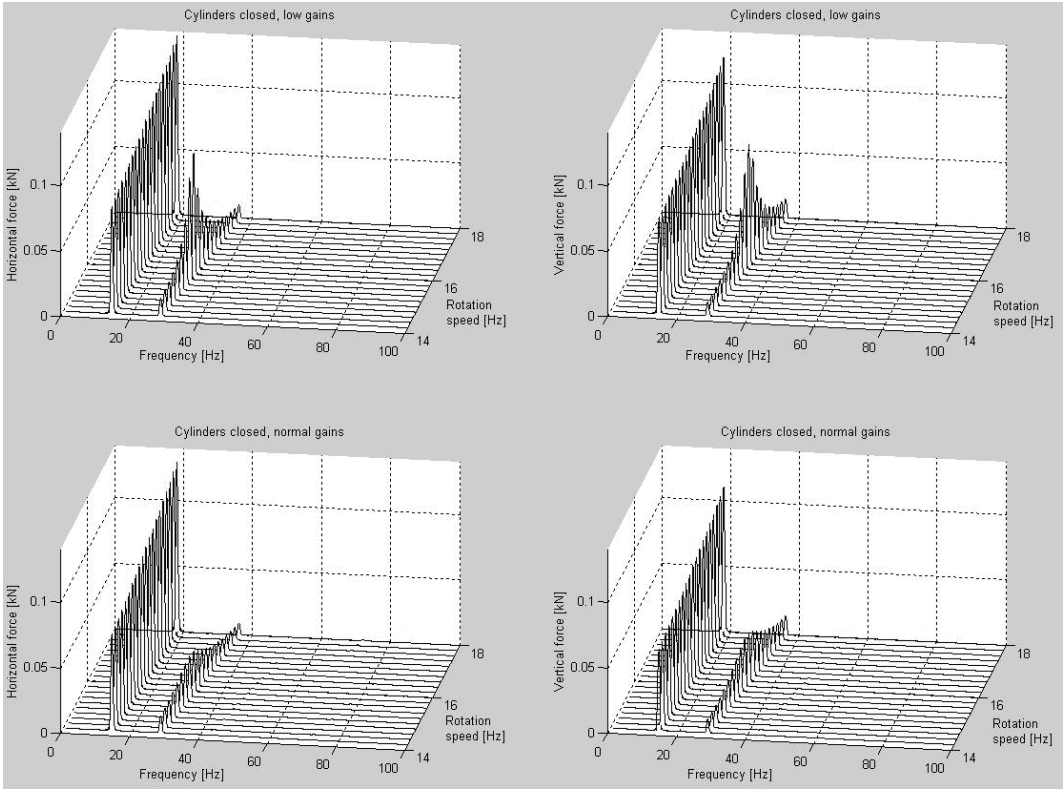

Figure 3: Spectrums of the horizontal (left) and vertical (right) forces generated by the three cylinders in the two cases, where the force PID controller has low gains (top row) and normal gains (bottom row). In the 'cylinders open' case the forces are constant.

Appendix D: Simplified Simulation of Active Damping with CC and HHC Algorithms

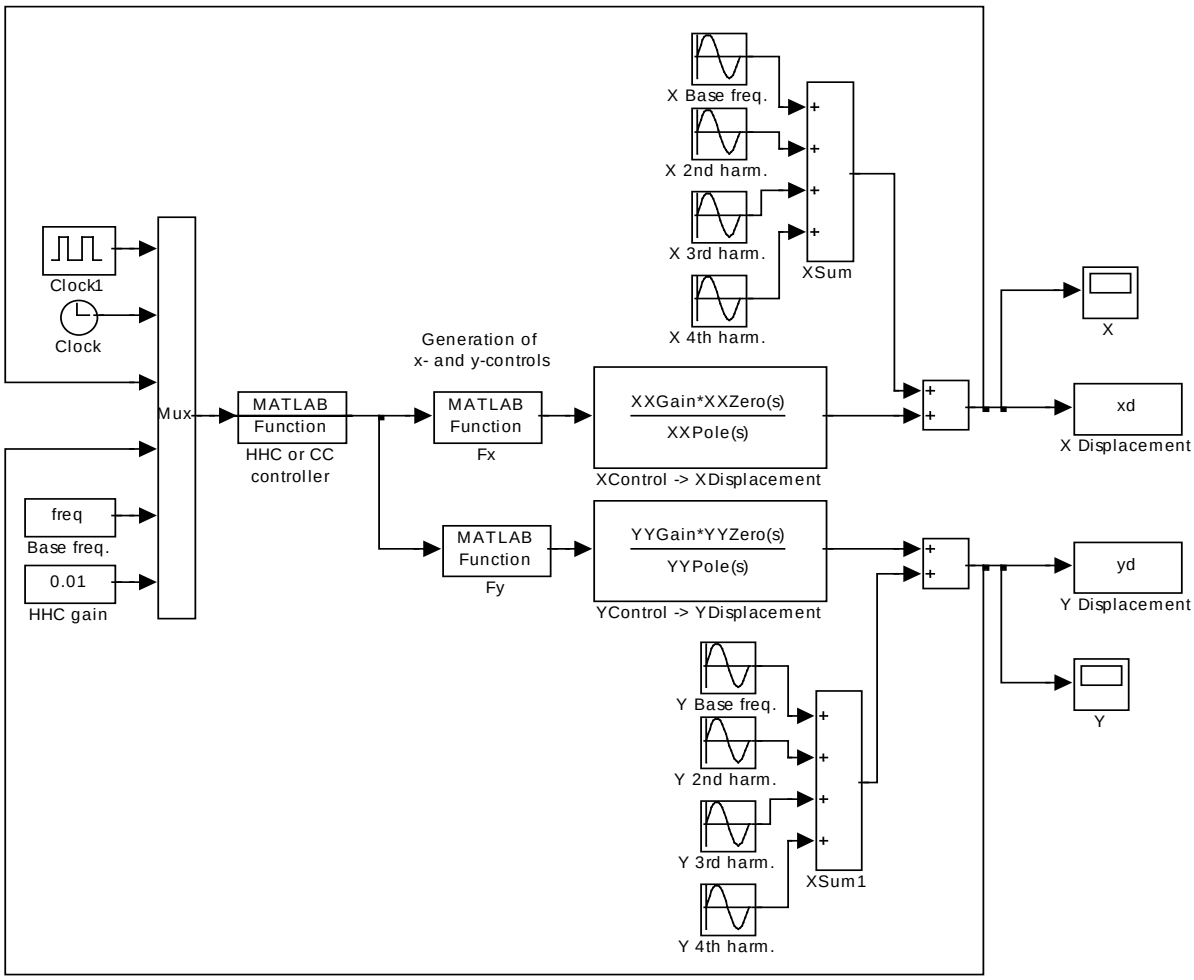

Figure 1: The simple Simulink simulation model. The horizontal and vertical models are transfer functions with given poles, zeros and gains. These models are the same, which are used in the CC or HHC algorithms, which are included as C-coded functions. The disturbance, which is to be damped, consists of four harmonic components with amplitudes 1, 0.2, 0.01 and 0.005. Since the damping algorithms are the same, which are used with ADAMS model, their outputs are control signals (force set values) for the three cylinders and these have to be transformed to horizontal and vertical controls before feeding to the transfer functions.

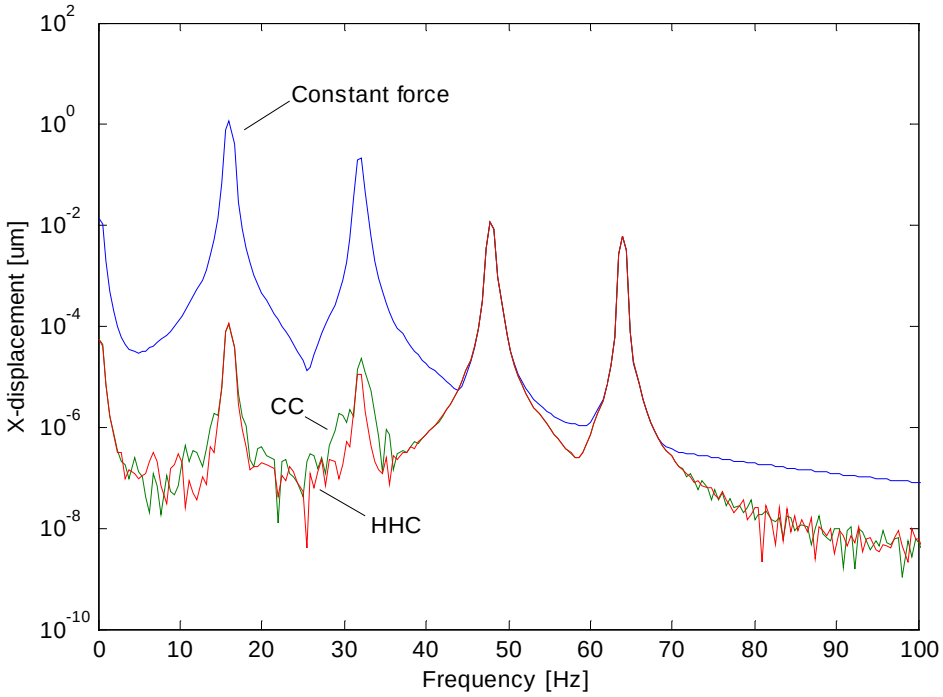

Figure 2: Damping the 1st and 2nd harmonic frequencies with the simple Simulink model. The base frequency is 16 Hz. The spectrums of the horizontal displacements in three cases: without active damping ('Constant force', blue line), with HHC damping ('HHC', red line) and with convergent control ('CC', green line).

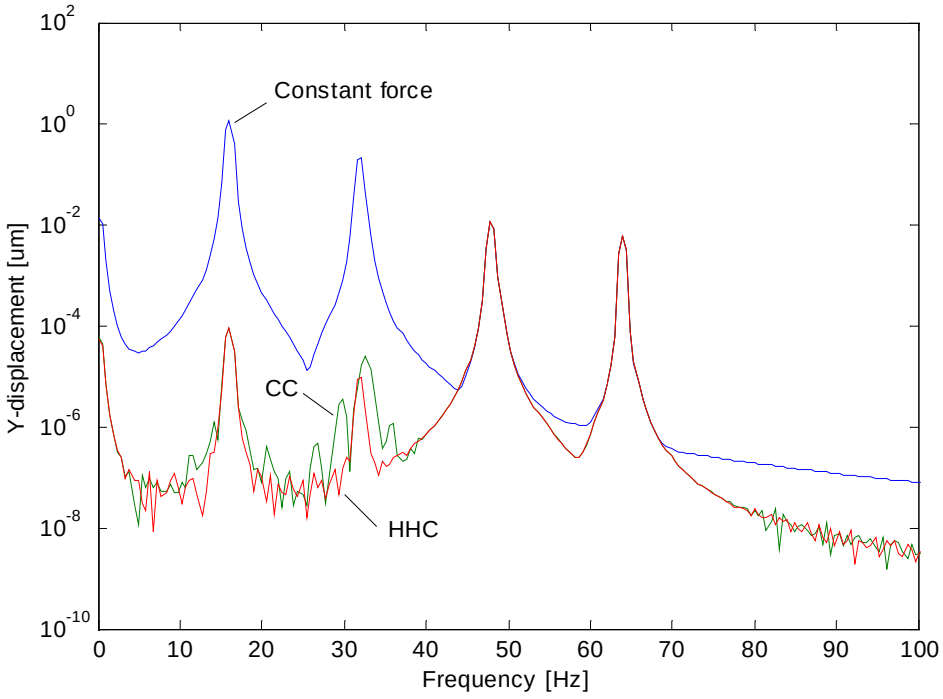

Figure 3: Damping the 1st and 2nd harmonic frequencies with the simple Simulink model. The base frequency 16 Hz. The spectrums of the vertical displacements in three cases: without active damping ('Constant force', blue line), with HHC damping ('HHC', red line) and with convergent control ('CC', green line).